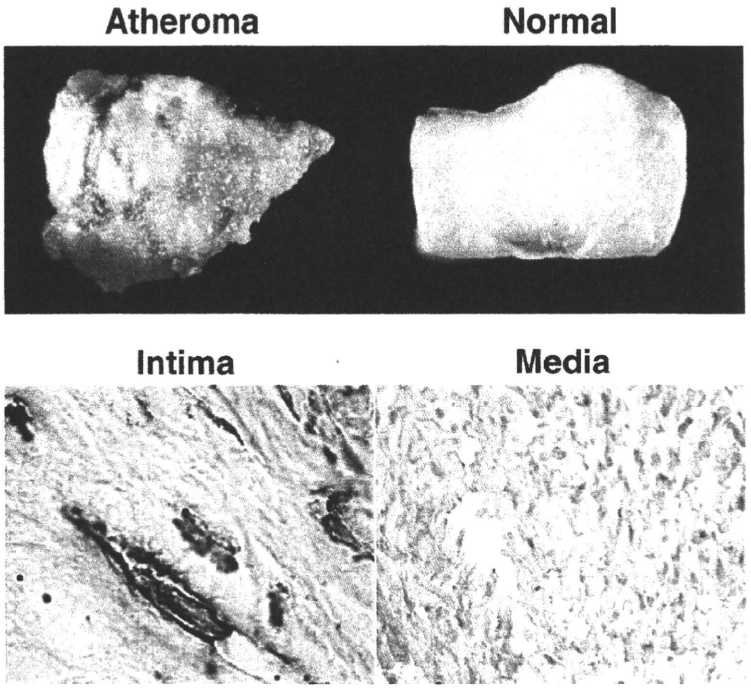

Figure 1. Senescent vascular cells in human atheroma. (**Upper panel**) Human atheroma (**Left**) and non-atherosclerotic arterial tissue (**Right**) were obtained from human carotid and internal mammary arteries, respectively, at autopsy and the luminal surfaces were stained with SAβ-gal. SAβ-gal activity can be seen in the atherosclerotic lesion but not in the normal lesion. (**Lower panel**) Double staining for SAβ-gal and α-smooth muscle actin in sections of human atheroma shown in the upper panel identified SAβ-gal positive cells as VSMCs in the intima but not in the media. SAβ-gal, senescence-associated β-galactosidase; VSMC, vascular smooth muscle cells. (Adapted from Minamino et al[11] with permission.)

breaks form in cells with critically short or dysfunctional telomeres,[15,16] and these telomere dysfunction-induced nuclear foci are increased in the fibroblasts of aging primates.[17]

It has been reported that telomere shortening occurs in human vessels and may be related to atherogenesis. Telomere length in ECs from the abdominal aorta and the iliac arteries shows a strong inverse correlation with age.[18,19] Interestingly, telomere shortening occurs faster in the endothelial cells of the iliac arteries than in those of the internal mammary arteries.[18] Thus, a high level of hemodynamic stress may enhance EC turnover in the iliac arteries compared with vessels subjected to less stress. Telomeres are shorter in coronary artery ECs from patients with coronary heart disease than in cells from healthy subjects.[20] A recent study demonstrated that endothelial telomere length was shorter in patients with a longer history of risk factors for cardiovascular disease,[21] suggesting that these factors override the effect of chronological aging on EC turnover by accelerating stress-induced damage. Identification of factors that accelerate endothelial telomere attrition will provide a novel target for the treatment of human atherosclerosis.

Role of Telomeres in Vascular Senescence

It has been demonstrated that disturbance of telomere integrity leads to endothelial dysfunction in vitro.[9] Human ECs and VSMCs express telomerase activity, which is markedly increased by mitogenic stimuli,[22] but this activity declines with aging because of decreased expression of the catalytic component of telomerase, leading to telomere shortening and cellular senescence.[23] Introduction of telomerase prevents endothelial dysfunction associated with senescence, including decreased eNOS activity and increased monocyte adhesion to ECs.[9,24] Immortalized human ECs have been established by introduction of telomerase, and these appear to retain EC characteristics, including various cell surface markers.[25] When cultured in Matrigel, they form capillary-like structures as efficiently as ECs from an early passage.[26]

Telomerase-deficient mice have a normal phenotype in the first generation, presumably because mice possess very long telomeres.[27,28] However, their telomeres become shorter with successive generations, and the mice become infertile by the 6th generation because of impairment of the reproductive system.[28] Some of the abnormalities in the later generations of these mice mimic age-associated changes. For example, these animals have a shortened lifespan and a reduced capacity to respond to stresses such as wounds and hematopoietic ablation.[29] Neovascularization is also impaired in the later generations of telomerase-deficient mice,[30] and their decreased ability to form new vessels may be attributed to impaired function and replication of vascular ECs induced by telomere shortening. In a mouse model of atherosclerosis, telomere shortening has been shown to decrease the area of atherosclerotic lesions, presumably because of the reduced proliferation of macrophages.[31] However, telomerase-deficient mice develop atherosclerotic plaques with a thin fibrous cap, suggesting that shortening of the telomeres in vascular cells may lead to plaque rupture in human atherosclerosis. Mice lacking telomerase activity develop hypertension in the 1st and 3rd generations as a result of an increased plasma endothelin-1 level caused by an overexpression of endothelin-converting enzyme.[32]

Stress-Induced Premature Senescence

In response to various stress signals, cells develop a phenotype indistinguishable from that of senescent cells at the end of their replicative life span. For example, the constitutive activation of mitogenic stimuli by expression of oncogenic Ras induces a senescent phenotype in vascular cells.[10] Cellu-

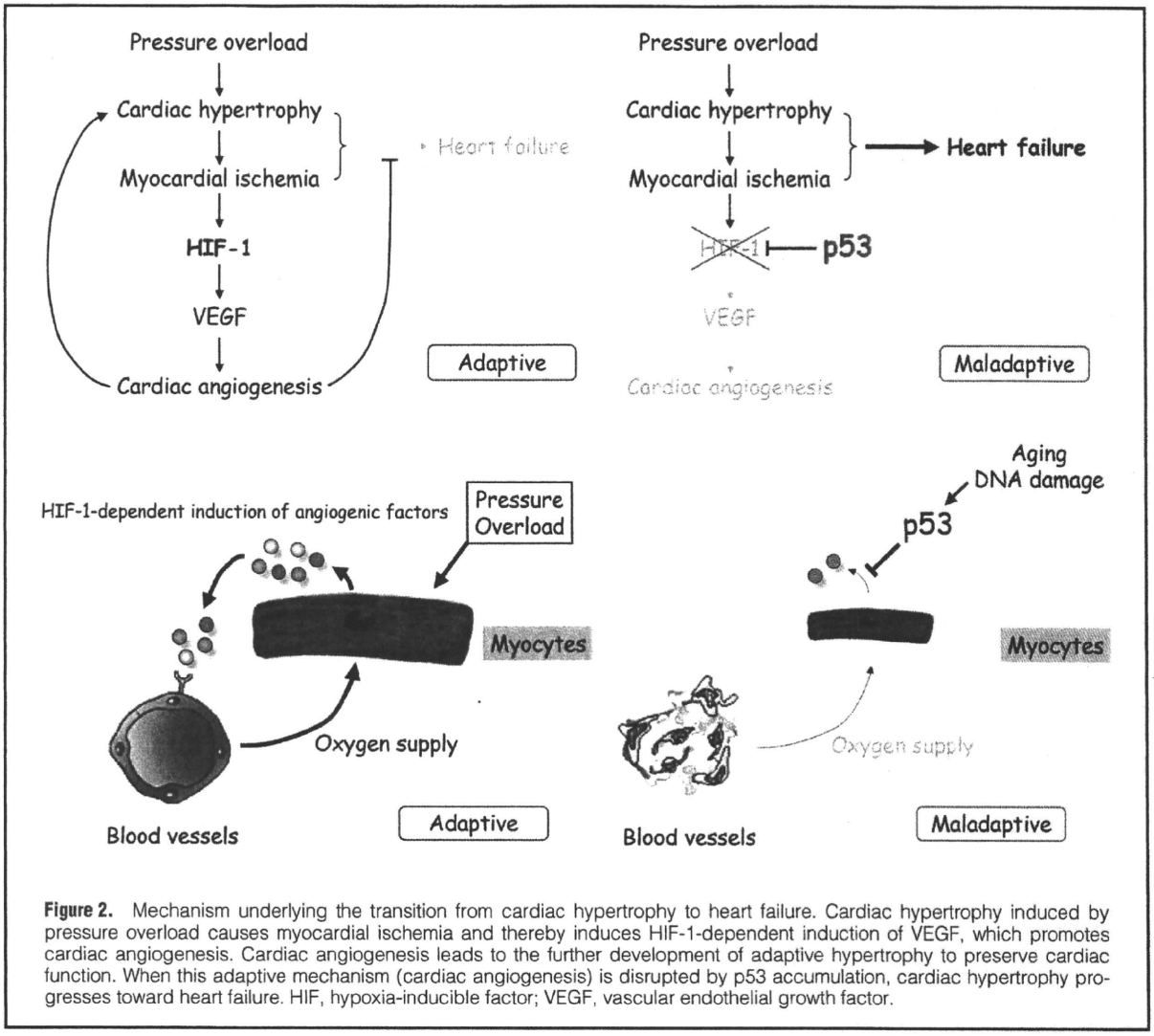

Figure 2. Mechanism underlying the transition from cardiac hypertrophy to heart failure. Cardiac hypertrophy induced by pressure overload causes myocardial ischemia and thereby induces HIF-1-dependent induction of VEGF, which promotes cardiac angiogenesis. Cardiac angiogenesis leads to the further development of adaptive hypertrophy to preserve cardiac function. When this adaptive mechanism (cardiac angiogenesis) is disrupted by p53 accumulation, cardiac hypertrophy progresses toward heart failure. HIF, hypoxia-inducible factor; VEGF, vascular endothelial growth factor.

lar senescence triggered by mitogenic stimuli is independent of replicative age, and these signals act before the replicative limits of cells. Hence, it is apparently telomere-independent and thus termed 'stress-induced premature senescence'. Arterial components of the angiotensin II (Ang II) signaling cascade increase with aging and contribute to the pathogenesis of atherosclerosis, and inhibition of Ang II activity has been demonstrated to improve the morbidity and mortality of cardiovascular disease.[33] Ang II has been reported to induce the premature senescence of human VSMCs via the p53/p21-dependent pathway.[34] Ang II was shown to increase the number of senescent VSMCs and induce the expression of proinflammatory molecules, as well as p21, in a mouse model of atherosclerosis.[34] Loss of p21 markedly ameliorated the induction of proinflammatory molecules by Ang II, thereby preventing the development of atherosclerosis.

Oxidative stress and DNA damage have been shown to induce premature senescence in vascular cells and have been suggested to contribute to atherogenesis.[34,35] There is also evidence that exposure to chronic oxidative stress, including oxidized low-density lipoprotein, enhances telomere shortening and accelerates the onset of senescence in human ECs.[36] Conversely, treatment with antioxidants preserves telomere length and extends the lifespan of ECs isolated from patients with severe coronary heart disease, unless the oxidative stress-induced damage becomes irreversible.[37] One of the cellular targets of oxidative stress is DNA. Many different types of oxidative DNA lesions have been described, ranging from base modifications to single- and double-strand breaks.[38] To cope with DNA damage, cells have evolved repair systems. Mice that lack components of these DNA repair systems exhibit the early onset of changes associated with aging, similar to their human counterparts,[38] and fibroblasts from these mice show accelerated senescence. Constitutive activation of p53[39,40] causes premature aging that is characterized by a reduced lifespan, osteoporosis, organ atrophy, and diminished stress tolerance. More importantly, cellular senescence has been detected in vivo by studies of mice with premature aging.[41] Together with the data from telomerase-deficient mice, these results provide in vivo evidence of a link between cellular senescence and aging of the organism.

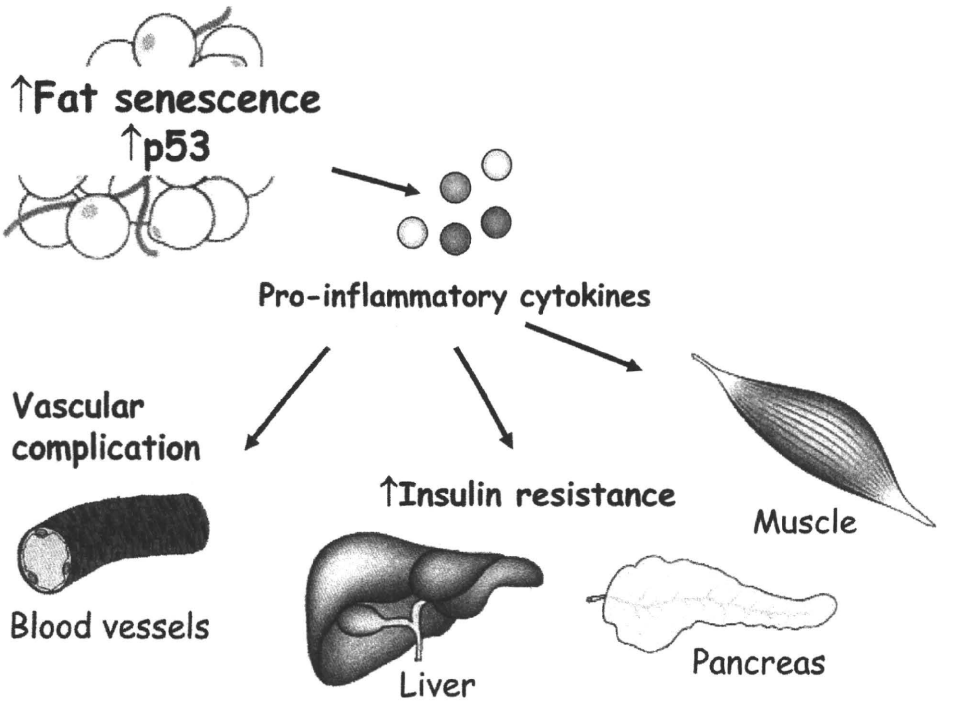

Figure 3. Role of adipose p53 in insulin resistance. Aging or excessive calorie intake leads to accumulation of p53 in adipose tissue, which upregulates the expression of proinflammatory molecules, thereby promoting the infiltration of macrophages. This leads to a further increase in the production of proinflammatory cytokines by adipose tissue, which induces insulin resistance, as well as vascular complications.

Cardiac Senescence

It has been reported that the number of myocytes declines with advancing age,[42] presumably because of apoptosis or necrosis, whereas human cardiomyocyte replication has been reported to occur in the failing heart, as well as in the infarcted heart,[43,44] suggesting that cardiac homeostasis could be regulated by the balance between myocyte loss and proliferation, and that aging impairs this equilibrium. In line with this notion, the number of myocytes with short telomeres is increased in the aging rat heart.[45] Likewise, telomere length is significantly reduced in the cells of the human failing heart compared with normal samples.[46] This reduction is enhanced with aging and associated with increased cardiac apoptosis, as well as activation of the DNA damage checkpoint kinase Chk2.[46] Later generations of telomerase-deficient mice show significant telomere shortening in myocytes, which is coupled with attenuation of myocyte proliferation and increased apoptosis.[47] These impairments are associated with ventricular dilatation and systolic dysfunction,[47] suggesting that telomere shortening with age could contribute to cardiac failure in the elderly. Cardiac telomerase activity declines with age, whereas forced expression of telomerase prevent age-associated telomere shortening, thereby promoting cardiomyocyte proliferation and survival.[48] Telomerase is detected mostly in cycling myocytes that express stem cell antigens, but also in proliferating myocytes without stem cell markers.[49] The number of these proliferative cardiomyocytes is increased in human cardiac hypertrophy[49] and ischemic heart failure,[50] however; regeneration of myocytes appears to be insufficient, resulting in systolic dysfunction. Recently, a genetic fate-mapping study has demonstrated that cardiac progenitor cells (CPC) participate in the formation of new cardiomyocytes after injury, but do not contribute to refreshment of uninjured cardiomyocytes during normal aging in mice.[51]

Accumulating evidence has suggested that aging or pathological stimuli promotes both senescence and apoptosis of CPC, thereby decreasing the number of functionally competent CPC.[52] For example, the number of p53- or p16-positive CPC with short telomeres is increased in the aged animal heart,[53] as well as in the human chronic ischemic heart.[50] Senescence of CPC is more prominent in old patients with a diseased heart.[54] In the hearts of diabetic subjects, increased oxidative stress leads to telomere shortening, upregulation of p53 and p16, and apoptosis of CPC, thereby compromising cardiac structure and function.[55] Together with senescent CPC, old non-replicating p53/p16-positive myocytes with short telomeres are increased in the aged heart, and these cells exhibits impaired contractile function.[53] Thus, impaired function of senescent CPCs appears to affect the refreshment of myocytes, and therefore senescent myocytes with poor contractility accumulate, leading to the development of aging myopathy. Activation of CPC by growth factors, such as insulin-like growth factor-1 and hepatocyte growth factor, has been shown to promote regeneration of cardiomyocytes, restoring the cardiac dysfunction associated with aging, suggesting that treatment with these growth factors may become an effective therapeutic strategy for myocardial aging.[53,56,57]

Cardiac hypertrophy is an adaptive response to increased workload in order to maintain cardiac function.[58] However, prolonged cardiac hypertrophy causes heart failure,[59–61] and the mechanisms are largely unknown. It was recently demonstrated that cardiac angiogenesis is critically involved in the adaptive mechanism of cardiac hypertrophy and that p53 accumulation is crucial for the transition from cardiac hypertrophy to heart failure. Pressure overload initially promotes vascular growth in the heart as a result of hypoxia-inducible factor-1 (HIF-1)-dependent induction of angiogenic factors, and inhibition of angiogenesis prevents the development of cardiac hypertrophy and induced systolic dysfunction. Sustained pressure overload induces accumulation of p53, which inhibits HIF-1 activity and thereby impairs cardiac angiogenesis and systolic function. Conversely, promoting cardiac angiogenesis by introducing angiogenic factors or by inhibiting p53 accumulation further develops hypertrophy and restores cardiac dysfunction under chronic pressure overload. These results suggest that the anti-angiogenic property of p53 plays a critical role in the transition from cardiac hypertrophy to heart failure (**Figure 2**).

Accumulation of p53 in the heart has been reported in aging and several diseases, such as diabetes,[47,62,63] which may be the reason older people and diabetic patients are susceptible to heart failure when chronic pressure overload develops. Thus, inhibition of p53 or promotion of vascular growth in the heart may be a novel therapeutic strategy to prevent the transition from cardiac hypertrophy to heart failure in aged people and diabetic patients.

Adipose Senescence and Diabetes

Aging is known to increase the prevalence of metabolic disorders such as diabetes. Therefore, it has been hypothesized that cellular aging might influence insulin resistance (IR) and accelerate the development of diabetes. Using various genetic models, including telomerase-deficient mice, it has been recently shown that p53 in adipose tissue is critically involved in IR, which underlies age-related cardiovascular and metabolic disorders.[64] Telomerase-deficient mice with short telomeres developed IR when fed a high-calorie diet. The adipose tissue of these mice showed senescence-like changes, such as increases in the activity of SAβ-gal, level of expression of p53, and production of proinflammatory cytokines. Resection of senescent adipose tissue improved IR in the telomerase-deficient mice, and implantation of senescent adipose tissue into wild-type mice led to impairment of insulin sensitivity and glucose tolerance in the recipients. Upregulation of p53 induced the expression of proinflammatory cytokines and accumulation of macrophages in adipose tissue. It was also found that excessive calorie intake led to the accumulation of oxidative stress in the adipose tissue of type 2 diabetic mice and promoted senescence-like changes, thereby increasing production of pro-inflammatory cytokines. Inhibition of p53 activity significantly ameliorated these senescence-like changes of adipose tissue, decreased the expression of proinflammatory cytokines, and improved IR in type 2 diabetic mice. Conversely, upregulation of p53 in adipose tissue caused an inflammatory response that led to IR. Adipose tissue from diabetic patients also shows senescence-like features. These findings indicate that cellular aging signals (particularly p53 in adipose tissue) upregulate the expression of proinflammatory molecules, thereby promoting the infiltration of macrophages into adipose tissue, which leads to a further increase in the production of proinflammatory cytokines by the adipose tissue, which induces IR and glucose intolerance (**Figure 3**). Our results demonstrate a previously unappreciated role of adipose-related p53 in the regulation of IR and suggest that cellular aging signals in adipose tissue could be a novel target for the treatment of diabetes.

Recent studies have shown that longevity signals in adipose tissue plays a crucial role in regulating the lifespan of various species, ranging from worms to mice, and suggested the existence of cellular non-autonomous regulation of aging by adipose tissue.[65–68] Consistent with those reports, subcutaneous implantation of senescent adipose tissue from telomerase-deficient mice accelerated the senescence of epididymal fat in wild-type recipients (T. Minamino, unpublished data). The senescence of adipose tissue may increase the local production of proinflammatory molecules, but may also promote systemic inflammation via cellular non-autonomous mechanisms. Low levels of circulating insulin are generally associated with longevity, and activation of longevity signals in adipose tissue has been reported to reduce the circulating insulin level and extend the lifespan.[69,70] It has been found that inhibition of p53 activity in adipose tissue improves IR and thus decreases the plasma insulin level. Thus, p53 activation in adipose tissue may be a pro-aging signal that negatively regulates longevity, so inhibition of cellular aging may become a novel therapeutic strategy for aging and its associated diseases.

Conclusions

Cell division is essential for the survival of multicellular organisms that contain renewable tissues, but places the organism at risk of developing cancer. Thus, complex organisms have evolved at least 2 cellular mechanisms to prevent oncogenic transformation: apoptosis and cellular senescence. In this regard, aging and age-associated diseases can be viewed as byproducts of the tumor suppressor mechanism known as cellular senescence. Consistent with this idea, the number of senescent fibroblasts increases exponentially in the skin of aging primates.[17] Conversely, extension of the lifespan by calorie restriction decreases biomarkers of cellular senescence in vivo.[71] We therefore need to identify the molecular mechanisms by which aging accelerates cellular aging in order to prevent the development of lifestyle-related diseases. Identification of such mechanisms could lead to a new treatment strategy for various age-associated diseases, such as neurodegenerative disease, as well as lifestyle-related diseases.

References

1. Campisi J. The biology of replicative senescence. *Eur J Cancer* 1997; **33:** 703–709.
2. Bringold F, Serrano M. Tumor suppressors and oncogenes in cellular senescence. *Exp Gerontol* 2000; **35:** 317–329.
3. Dimri GP, Lee X, Basile G, Acosta M, Scott G, Roskelley C, et al. A biomarker that identifies senescent human cells in culture and in aging skin in vivo. *Proc Natl Acad Sci USA* 1995; **92:** 9363–9367.
4. Kumazaki T, Kobayashi M, Mitsui Y. Enhanced expression of fibronectin during in vivo cellular aging of human vascular endothelial cells and skin fibroblasts. *Exp Cell Res* 1993; **205:** 396–402.
5. Bennett MR, Macdonald K, Chan SW, Boyle JJ, Weissberg PL. Cooperative interactions between RB and p53 regulate cell proliferation, cell senescence, and apoptosis in human vascular smooth muscle cells from atherosclerotic plaques. *Circ Res* 1998; **82:** 704–712.
6. Burrig KF. The endothelium of advanced arteriosclerotic plaques in humans. *Arterioscler Thromb* 1991; **11:** 1678–1689.
7. Ross R, Wight TN, Strandness E, Thiele B. Human atherosclerosis. I: Cell constitution and characteristics of advanced lesions of the superficial femoral artery. *Am J Pathol* 1984; **114:** 79–93.

8. Fenton M, Barker S, Kurz DJ, Erusalimsky JD. Cellular senescence after single and repeated balloon catheter denudations of rabbit carotid arteries. *Arterioscler Thromb Vasc Biol* 2001; **21:** 220–226.
9. Minamino T, Miyauchi H, Yoshida T, Ishida Y, Yoshida H, Komuro I. Endothelial cell senescence in human atherosclerosis: Role of telomere in endothelial dysfunction. *Circulation* 2002; **105:** 1541–1544.
10. Minamino T, Yoshida T, Tateno K, Miyauchi H, Zou Y, Toko H, et al. Ras induces vascular smooth muscle cell senescence and inflammation in human atherosclerosis. *Circulation* 2003; **108:** 2264–2269.
11. Minamino T, Miyauchi H, Yoshida T, Tateno K, Kunieda T, Komuro I. Vascular cell senescence and vascular aging. *J Mol Cell Cardiol* 2004; **36:** 175–183.
12. Vanhoutte PM. Endothelial dysfunction: The first step toward coronary arteriosclerosis. *Circ J* 2009; **73:** 595–601.
13. Blasco MA. Telomeres and human disease: Ageing, cancer and beyond. *Nat Rev Genet* 2005; **6:** 611–622.
14. Herbig U, Jobling WA, Chen BP, Chen DJ, Sedivy JM. Telomere shortening triggers senescence of human cells through a pathway involving ATM, p53, and p21(CIP1), but not p16(INK4a). *Mol Cell* 2004; **14:** 501–513.
15. d'Adda di Fagagna F, Reaper PM, Clay-Farrace L, Fiegler H, Carr P, Von Zglinicki T, et al. A DNA damage checkpoint response in telomere-initiated senescence. *Nature* 2003; **426:** 194–198.
16. Takai H, Smogorzewska A, de Lange T. DNA damage foci at dysfunctional telomeres. *Curr Biol* 2003; **13:** 1549–1556.
17. Herbig U, Ferreira M, Condel L, Carey D, Sedivy JM. Cellular senescence in aging primates. *Science* 2006; **311:** 1257.
18. Chang E, Harley CB. Telomere length and replicative aging in human vascular tissues. *Proc Natl Acad Sci USA* 1995; **92:** 11190–11194.
19. Aviv H, Khan MY, Skurnick J, Okuda K, Kimura M, Gardner J, et al. Age dependent aneuploidy and telomere length of the human vascular endothelium. *Atherosclerosis* 2001; **159:** 281–287.
20. Ogami M, Ikura Y, Ohsawa M, Matsuo T, Kayo S, Yoshimi N, et al. Telomere shortening in human coronary artery diseases. *Arterioscler Thromb Vasc Biol* 2004; **24:** 546–550.
21. Voghel G, Thorin-Trescases N, Farhat N, Nguyen A, Villeneuve L, Mamarbachi AM, et al. Cellular senescence in endothelial cells from atherosclerotic patients is accelerated by oxidative stress associated with cardiovascular risk factors. *Mech Ageing Dev* 2007; **128:** 662–671.
22. Minamino T, Kourembanas S. Mechanisms of telomerase induction during vascular smooth muscle cell proliferation. *Circ Res* 2001; **89:** 237–243.
23. Minamino T, Mitsialis SA, Kourembanas S. Hypoxia extends the life span of vascular smooth muscle cells through telomerase activation. *Mol Cell Biol* 2001; **21:** 3336–3342.
24. Matsushita H, Chang E, Glassford AJ, Cooke JP, Chiu CP, Tsao PS. eNOS activity is reduced in senescent human endothelial cells: Preservation by hTERT immortalization. *Circ Res* 2001; **89:** 793–798.
25. Yang J, Chang E, Cherry AM, Bangs CD, Oei Y, Bodnar A, et al. Human endothelial cell life extension by telomerase expression. *J Biol Chem* 1999; **274:** 26141–26148.
26. Yang J, Nagavarapu U, Relloma K, Sjaastad MD, Moss WC, Passaniti A, et al. Telomerized human microvasculature is functional in vivo. *Nat Biotechnol* 2001; **19:** 219–224.
27. Blasco MA, Lee HW, Hande MP, Samper E, Lansdorp PM, DePinho RA, et al. Telomere shortening and tumor formation by mouse cells lacking telomerase RNA. *Cell* 1997; **91:** 25–34.
28. Lee HW, Blasco MA, Gottlieb GJ, Horner JW 2nd, Greider CW, DePinho RA. Essential role of mouse telomerase in highly proliferative organs. *Nature* 1998; **392:** 569–574.
29. Rudolph KL, Chang S, Lee HW, Blasco M, Gottlieb GJ, Greider C, et al. Longevity, stress response, and cancer in aging telomerase-deficient mice. *Cell* 1999; **96:** 701–712.
30. Franco S, Segura I, Riese HH, Blasco MA. Decreased B16F10 melanoma growth and impaired vascularization in telomerase-deficient mice with critically short telomeres. *Cancer Res* 2002; **62:** 552–559.
31. Poch E, Carbonell P, Franco S, Diez-Juan A, Blasco MA, Andres V. Short telomeres protect from diet-induced atherosclerosis in apolipoprotein E-null mice. *Faseb J* 2004; **18:** 418–420.
32. Perez-Rivero G, Ruiz-Torres MP, Rivas-Elena JV, Jerkic M, Diez-Marques ML, Lopez-Novoa JM, et al. Mice deficient in telomerase activity develop hypertension because of an excess of endothelin production. *Circulation* 2006; **114:** 309–317.
33. Najjar SS, Scuteri A, Lakatta EG. Arterial aging: Is it an immutable cardiovascular risk factor? *Hypertension* 2005; **46:** 454–462.
34. Kunieda T, Minamino T, Nishi J, Tateno K, Oyama T, Katsuno T, et al. Angiotensin II induces premature senescence of vascular smooth muscle cells and accelerates the development of atherosclerosis via a p21-dependent pathway. *Circulation* 2006; **114:** 953–960.
35. Matthews C, Gorenne I, Scott S, Figg N, Kirkpatrick P, Ritchie A, et al. Vascular smooth muscle cells undergo telomere-based senescence in human atherosclerosis: Effects of telomerase and oxidative stress. *Circ Res* 2006; **99:** 156–164.
36. Kurz DJ, Decary S, Hong Y, Trivier E, Akhmedov A, Erusalimsky JD. Chronic oxidative stress compromises telomere integrity and accelerates the onset of senescence in human endothelial cells. *J Cell Sci* 2004; **117:** 2417–2426.
37. Voghel G, Thorin-Trescases N, Farhat N, Mamarbachi AM, Villeneuve L, Fortier A, et al. Chronic treatment with N-acetylcystein delays cellular senescence in endothelial cells isolated from a subgroup of atherosclerotic patients. *Mech Ageing Dev* 2008; **129:** 261–270.
38. Hasty P, Campisi J, Hoeijmakers J, van Steeg H, Vijg J. Aging and genome maintenance: Lessons from the mouse? *Science* 2003; **299:** 1355–1359.
39. Tyner SD, Venkatachalam S, Choi J, Jones S, Ghebranious N, Igelmann H, et al. p53 mutant mice that display early ageing-associated phenotypes. *Nature* 2002; **415:** 45–53.
40. Maier B, Gluba W, Bernier B, Turner T, Mohammad K, Guise T, et al. Modulation of mammalian life span by the short isoform of p53. *Genes Dev* 2004; **18:** 306–319.
41. Cao L, Li W, Kim S, Brodie SG, Deng CX. Senescence, aging, and malignant transformation mediated by p53 in mice lacking the Brca1 full-length isoform. *Genes Dev* 2003; **17:** 201–213.
42. Olivetti G, Giordano G, Corradi D, Melissari M, Lagrasta C, Gambert SR, et al. Gender differences and aging: Effects on the human heart. *J Am Coll Cardiol* 1995; **26:** 1068–1079.
43. Kajstura J, Leri A, Finato N, Di Loreto C, Beltrami CA, Anversa P. Myocyte proliferation in end-stage cardiac failure in humans. *Proc Natl Acad Sci USA* 1998; **95:** 8801–8805.
44. Beltrami AP, Urbanek K, Kajstura J, Yan SM, Finato N, Bussani R, et al. Evidence that human cardiac myocytes divide after myocardial infarction. *N Engl J Med* 2001; **344:** 1750–1757.
45. Kajstura J, Pertoldi B, Leri A, Beltrami CA, Deptala A, Darzynkiewicz Z, et al. Telomere shortening is an in vivo marker of myocyte replication and aging. *Am J Pathol* 2000; **156:** 813–819.
46. Oh H, Wang SC, Prahash A, Sano M, Moravec CS, Taffet GE, et al. Telomere attrition and Chk2 activation in human heart failure. *Proc Natl Acad Sci USA* 2003; **100:** 5378–5383.
47. Leri A, Franco S, Zacheo A, Barlucchi L, Chimenti S, Limana F, et al. Ablation of telomerase and telomere loss leads to cardiac dilatation and heart failure associated with p53 upregulation. *EMBO J* 2003; **22:** 131–139.
48. Oh H, Taffet GE, Youker KA, Entman ML, Overbeek PA, Michael LH, et al. Telomerase reverse transcriptase promotes cardiac muscle cell proliferation, hypertrophy, and survival. *Proc Natl Acad Sci USA* 2001; **98:** 10308–10313.
49. Urbanek K, Quaini F, Tasca G, Torella D, Castaldo C, Nadal-Ginard B, et al. Intense myocyte formation from cardiac stem cells in human cardiac hypertrophy. *Proc Natl Acad Sci USA* 2003; **100:** 10440–10445.
50. Urbanek K, Torella D, Sheikh F, De Angelis A, Nurzynska D, Silvestri F, et al. Myocardial regeneration by activation of multipotent cardiac stem cells in ischemic heart failure. *Proc Natl Acad Sci USA* 2005; **102:** 8692–8697.
51. Hsieh PC, Segers VF, Davis ME, MacGillivray C, Gannon J, Molkentin JD, et al. Evidence from a genetic fate-mapping study that stem cells refresh adult mammalian cardiomyocytes after injury. *Nat Med* 2007; **13:** 970–974.
52. Hosoda T, Kajstura J, Leri A, Anversa P. Mechanisms of myocardial regeneration. *Circ J* 2010; **74:** 13–17.
53. Torella D, Rota M, Nurzynska D, Musso E, Monsen A, Shiraishi I, et al. Cardiac stem cell and myocyte aging, heart failure, and insulin-like growth factor-1 overexpression. *Circ Res* 2004; **94:** 514–524.
54. Chimenti C, Kajstura J, Torella D, Urbanek K, Heleniak H, Colussi C, et al. Senescence and death of primitive cells and myocytes lead to premature cardiac aging and heart failure. *Circ Res* 2003; **93:** 604–613.
55. Rota M, LeCapitaine N, Hosoda T, Boni A, De Angelis A, Padin-Iruegas ME, et al. Diabetes promotes cardiac stem cell aging and heart failure, which are prevented by deletion of the p66shc gene. *Circ Res* 2006; **99:** 42–52.

56. Urbanek K, Rota M, Cascapera S, Bearzi C, Nascimbene A, De Angelis A, et al. Cardiac stem cells possess growth factor-receptor systems that after activation regenerate the infarcted myocardium, improving ventricular function and long-term survival. *Circ Res* 2005; **97:** 663–673.
57. Gonzalez A, Rota M, Nurzynska D, Misao Y, Tillmanns J, Ojaimi C, et al. Activation of cardiac progenitor cells reverses the failing heart senescent phenotype and prolongs lifespan. *Circ Res* 2008; **102:** 597–606.
58. Frey N, Olson EN. Cardiac hypertrophy: The good, the bad, and the ugly. *Annu Rev Physiol* 2003; **65:** 45–79.
59. Levy D, Garrison RJ, Savage DD, Kannel WB, Castelli WP. Prognostic implications of echocardiographically determined left ventricular mass in the Framingham Heart Study. *N Engl J Med* 1990; **322:** 1561–1566.
60. Ferrari R, Ceconi C, Campo G, Cangiano E, Cavazza C, Secchiero P, et al. Mechanisms of remodelling: A question of life (stem cell production) and death (myocyte apoptosis). *Circ J* 2009; **73:** 1973–1982.
61. Misra A, Mann DL. Treatment of heart failure beyond practice guidelines: Role of cardiac remodeling. *Circ J* 2008; **72**(Suppl A)**:** A-1–A-7.
62. Fiordaliso F, Leri A, Cesselli D, Limana F, Safai B, Nadal-Ginard B, et al. Hyperglycemia activates p53 and p53-regulated genes leading to myocyte cell death. *Diabetes* 2001; **50:** 2363–2375.
63. Kajstura J, Fiordaliso F, Andreoli AM, Li B, Chimenti S, Medow MS, et al. IGF-1 overexpression inhibits the development of diabetic cardiomyopathy and angiotensin II-mediated oxidative stress. *Diabetes* 2001; **50:** 1414–1424.
64. Minamino T, Orimo M, Shimizu I, Kunieda T, Yokoyama M, Ito T, et al. A crucial role for adipose tissue p53 in the regulation of insulin resistance. *Nat Med* 2009; **15:** 1082–1087.
65. Kenyon C. The plasticity of aging: Insights from long-lived mutants. *Cell* 2005; **120:** 449–460.
66. Hwangbo DS, Gershman B, Tu MP, Palmer M, Tatar M. Drosophila dFOXO controls lifespan and regulates insulin signalling in brain and fat body. *Nature* 2004; **429:** 562–566.
67. Giannakou ME, Goss M, Junger MA, Hafen E, Leevers SJ, Partridge L. Long-lived *Drosophila* with overexpressed dFOXO in adult fat body. *Science* 2004; **305:** 361.
68. Bluher M, Kahn BB, Kahn CR. Extended longevity in mice lacking the insulin receptor in adipose tissue. *Science* 2003; **299:** 572–574.
69. Bluher M, Michael MD, Peroni OD, Ueki K, Carter N, Kahn BB, et al. Adipose tissue selective insulin receptor knockout protects against obesity and obesity-related glucose intolerance. *Dev Cell* 2002; **3:** 25–38.
70. Libina N, Berman JR, Kenyon C. Tissue-specific activities of C. elegans DAF-16 in the regulation of lifespan. *Cell* 2003; **115:** 489–502.
71. Krishnamurthy J, Torrice C, Ramsey MR, Kovalev GI, Al-Regaiey K, Su L, et al. Ink4a/Arf expression is a biomarker of aging. *J Clin Invest* 2004; **114:** 1299–1307.

Excessive cardiac insulin signaling exacerbates systolic dysfunction induced by pressure overload in rodents

Ippei Shimizu,[1] Tohru Minamino,[1,2] Haruhiro Toko,[1] Sho Okada,[1] Hiroyuki Ikeda,[1] Noritaka Yasuda,[1] Kaoru Tateno,[1] Junji Moriya,[1] Masataka Yokoyama,[1] Aika Nojima,[1] Gou Young Koh,[3] Hiroshi Akazawa,[1] Ichiro Shiojima,[4] C. Ronald Kahn,[5] E. Dale Abel,[6] and Issei Komuro[1,4]

[1]Department of Cardiovascular Science and Medicine, Chiba University Graduate School of Medicine, Chiba, Japan. [2]PRESTO, Japan Science and Technology Agency, Saitama, Japan. [3]Biomedical Research Center and Biological Sciences, Korea Advanced Institute of Science and Technology, Daejeon, Korea. [4]Department of Cardiovascular Medicine, Osaka University School of Medicine, Osaka, Japan. [5]Joslin Diabetes Center, Harvard Medical School, Boston, Massachusetts, USA. [6]Division of Endocrinology, Metabolism and Diabetes and Program in Molecular Medicine, University of Utah School of Medicine, Salt Lake City, Utah, USA.

Although many animal studies indicate insulin has cardioprotective effects, clinical studies suggest a link between insulin resistance (hyperinsulinemia) and heart failure (HF). Here we have demonstrated that excessive cardiac insulin signaling exacerbates systolic dysfunction induced by pressure overload in rodents. Chronic pressure overload induced hepatic insulin resistance and plasma insulin level elevation. In contrast, cardiac insulin signaling was upregulated by chronic pressure overload because of mechanical stretch–induced activation of cardiomyocyte insulin receptors and upregulation of insulin receptor and Irs1 expression. Chronic pressure overload increased the mismatch between cardiomyocyte size and vascularity, thereby inducing myocardial hypoxia and cardiomyocyte death. Inhibition of hyperinsulinemia substantially improved pressure overload–induced cardiac dysfunction, improving myocardial hypoxia and decreasing cardiomyocyte death. Likewise, the cardiomyocyte-specific reduction of insulin receptor expression prevented cardiac ischemia and hypertrophy and attenuated systolic dysfunction due to pressure overload. Conversely, treatment of type 1 diabetic mice with insulin improved hyperglycemia during pressure overload, but increased myocardial ischemia and cardiomyocyte death, thereby inducing HF. Promoting angiogenesis restored the cardiac dysfunction induced by insulin treatment. We therefore suggest that the use of insulin to control hyperglycemia could be harmful in the setting of pressure overload and that modulation of insulin signaling is crucial for the treatment of HF.

Introduction

Cardiac hypertrophy is defined as an increment of ventricular mass resulting from increased cardiomyocyte size and is the adaptive response of the heart to an increased hemodynamic load due to either physiological factors such as exercise or pathological states such as hypertension and valvular diseases (1). Exercise-induced cardiac hypertrophy does not progress to heart failure (HF) (2, 3) and therefore is thought to be "physiological hypertrophy." On the other hand, pressure overload initially induces "adaptive hypertrophy," but causes "maladaptive (pathological) hypertrophy" in the chronic phase that results in HF (1).

Several signaling pathways have been implicated in the development of physiological or pathological cardiac hypertrophy. The insulin/PI3K/Akt axis plays a crucial role in the development of physiological hypertrophy as well as in normal cardiac growth, whereas activation of G-protein–coupled receptors in collaboration with PKC and calcineurin/nuclear factor of activated T cells (NFAT) pathways is involved in the development of pathological hypertrophy (4). Although homozygous cardiomyocyte-specific insulin receptor knockout (CIRKO) mice have smaller hearts than WT controls (5), both WT and CIRKO mice have shown a comparable increase of cardiac mass in response to pathological hypertrophic stimuli such as pressure overload (6). Overexpression of constitutively active p110α, a catalytic component of PI3K, in the heart has led to enhanced cardiac growth with preserved systolic function (7). Conversely, myocardial expression of dominant-negative p110α has inhibited the physiological hypertrophic response during postnatal growth and following exercise in mice, whereas the response to pressure overload has not been altered (8). Likewise, homozygous *Akt1*-deficient mice have shown defective exercise-induced cardiac hypertrophy (9), further supporting a crucial role of the insulin/PI3K/Akt pathway in physiological hypertrophy and growth of the heart.

Besides their role in physiological hypertrophy and normal cardiac growth, insulin signals may induce pathological hypertrophic responses. It has been shown that chronic hyperinsulinemia stimulates angiotensin II signaling that is involved in pathological hypertrophy (10). Mild to moderate activation of Akt was shown to induce cardiac hypertrophy with preservation of function (11, 12), whereas high levels of activated Akt expression in the heart led to pathological hypertrophy (13). Short-term Akt activation induced physiological cardiac hypertrophy, but constitutive activation of this pathway led to cardiac dysfunction (14). In this state, coordinated tissue growth and angiogenesis in the heart were disrupted, leading to myocardial hypoxia (14). Likewise, it has been demonstrated that chronic pressure overload increases the mismatch between cardiomyocyte size and vascularity and therefore induces

Authorship note: Ippei Shimizu and Tohru Minamino contributed equally to this work.

Conflict of interest: The authors have declared that no conflict of interest exists.

Citation for this article: *J Clin Invest.* 2010;120(5):1506–1514. doi:10.1172/JCI40096.

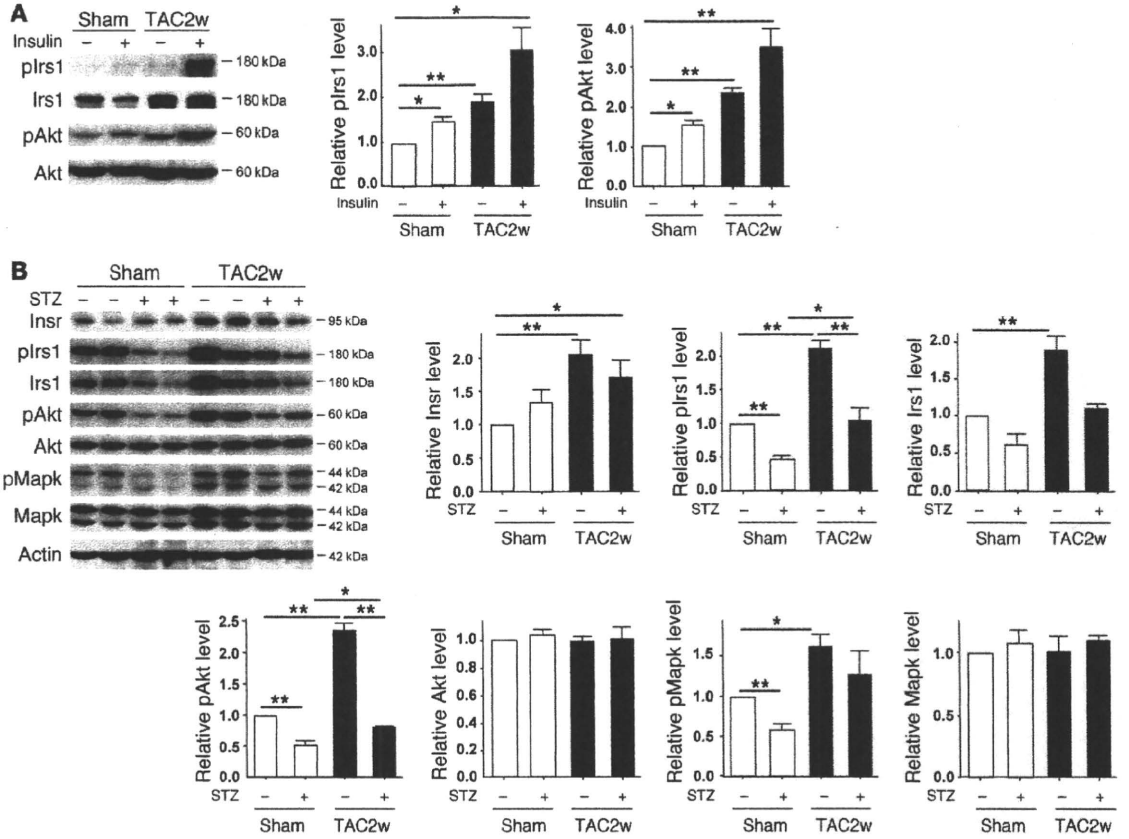

Figure 1

Upregulation of cardiac insulin signals by pressure overload. (**A**) Mice were subjected to TAC or sham operation (sham), and heart samples were obtained 2 weeks later. Mice were starved for 6 hours, and insulin or PBS was injected before sacrifice. pIrs1 and pAkt levels in the heart were examined by Western blot analysis. The graphs indicate relative expression levels of pIrs1 and pAkt. $n = 3$. TAC2w, 2 weeks after TAC. (**B**) Mice were subjected to TAC or sham operation and were sacrificed 2 weeks later. Components of the insulin signaling pathway in the heart were examined by Western blot analysis. The graphs indicate relative expression levels of these signaling molecules. $n = 3$. Data are shown as mean ± SEM. $^*P < 0.05$; $^{**}P < 0.01$.

myocardial hypoxia and cardiomyocyte death, leading to cardiac dysfunction (15). Moreover, intensive glycemic control of diabetic patients by insulin treatment has been reported to increase cardiovascular events (16). In the present study, we examined the role of insulin signaling in the development of cardiac dysfunction induced by pressure overload.

Results

Cardiac insulin signaling is activated by pressure overload. To investigate the role of the insulin signal pathway in failing hearts, we created severe transverse aortic constriction (TAC) in mice at 11 weeks of age. In this model, cardiac hypertrophy gradually progressed and reached a peak on day 7 after TAC (Supplemental Figure 1; supplemental material available online with this article; doi:10.1172/JCI40096DS1). Systolic function was preserved until day 7 but was significantly decreased on day 14 along with left ventricular dilatation (Supplemental Figure 1). Seven and fourteen days after TAC, we treated the mice with insulin (1 IU/kg) before sacrifice and examined the downstream signaling pathway of the insulin receptor (Insr) in the heart. Insulin-induced phosphorylation of insulin receptor substrate-1 (pIrs1) and Akt (pAkt) was markedly upregulated in the hearts of the TAC group compared with the sham-operated group (Figure 1A and Supplemental Figure 2A). We also found that the insulin signal pathway was constitutively activated in the TAC hearts under fasting conditions (Figure 1B and Supplemental Figure 2B). Expression of Insr and Irs1 protein as well as pIrs1 and pAkt protein was significantly increased in the TAC heart. These results suggest that chronic pressure overload upregulates cardiac insulin signaling. Enhanced insulin signaling was also observed in the hearts of spontaneously hypertensive rats (Supplemental Figure 3A).

Reduction of plasma insulin ameliorates systolic dysfunction induced by pressure overload. To determine whether upregulation of cardiac insulin signals has a pathological role in HF, we treated the mice with streptozotocin (STZ) (50 mg/kg i.p. for 5 days) at 4 weeks before TAC. Injection of STZ markedly decreased plasma insulin to below detectable levels, while the plasma glucose level gradually increased (Supplemental Figure 4). Pressure overload led to prominent cardiac hypertrophy along with upregulation of cardiac insulin signaling (Figure 1B and Figure 2, A and B). Systolic function was impaired and the left ventricular systolic dimension

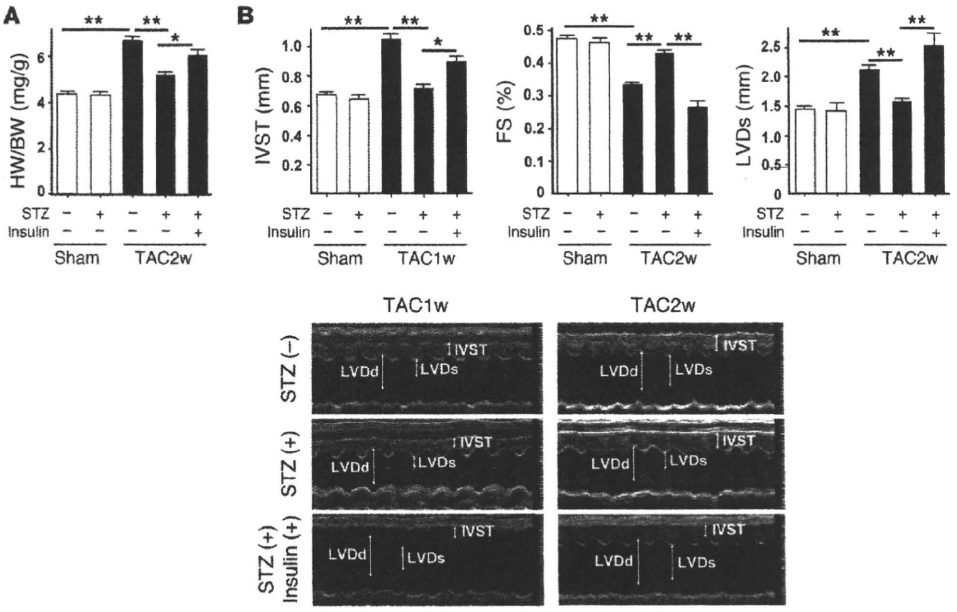

Figure 2

Depletion of plasma insulin attenuates systolic dysfunction induced by pressure overload. (**A**) STZ- or vehicle-treated mice were subjected to TAC or sham operation. The heart weight/body weight (HW/BW) ratio was measured 2 weeks after operation. In the insulin-treated group, daily i.p. injection of insulin (0.1 IU/g/d) was performed from 9 weeks (2 weeks after STZ treatment) to 13 weeks of age (2 weeks after TAC). n = 22–24. (**B**) Cardiac hypertrophy and systolic function of the animals prepared for **A** were estimated by echocardiography at 1 week (IVST) or 2 weeks (FS and LVDs) after operation. Photographs show representative results of echocardiography (M-mode). n = 6–10. Data are shown as mean ± SEM. $^*P < 0.05$; $^{**}P < 0.01$. IVST, intraventricular septal thickness; FS, fractional shortening.

(LVDs) was increased at 14 days after TAC (Figure 2, A and B). These alterations were significantly ameliorated in the mice treated with STZ (Figure 1B and Figure 2, A and B). Similar results were obtained at 6 weeks after TAC (Supplemental Figure 2C). We next examined the effect of insulin on cardiac function in this setting. STZ-treated mice were subjected to daily injection of insulin (0.1 IU/g/d from 9 weeks to 13 weeks of age) and to TAC at 11 weeks of age. Insulin treatment significantly improved hyperglycemia (Supplemental Figure 4). However, this treatment significantly enhanced cardiac hypertrophy and decreased systolic function along with left ventricular dilatation (Figure 2, A and B), indicating that insulin signaling influenced the development of systolic dysfunction due to pressure overload.

Reduction of plasma insulin inhibits cardiac hypoxia during pressure overload. We have recently demonstrated that cardiac angiogenesis is critically involved in the adaptive mechanism of cardiac hypertrophy and that an increased mismatch between cardiomyocyte size and vascularity is a crucial determinant of the transition from cardiac hypertrophy to HF (15). Consistent with our previous results, chronic pressure overload increased the cross-sectional area (CSA) of cardiomyocytes and decreased the relative vascularity (number of vessels/number of cardiomyocytes/CSA) (Figure 3, A–C), which in turn led to exacerbation of myocardial hypoxia (Figure 3D) and cardiomyocyte death (Figure 3E). In contrast, the increase of CSA after TAC was significantly attenuated by STZ treatment and the relative vascular density was markedly increased (Figure 3, A–C). Consequently, depletion of plasma insulin prevented cardiac hypoxia and cardiomyocyte death during chronic pressure overload (Figure 3, D and E). Conversely, insulin treatment of STZ-treated mice increased CSA and decreased relative vascular density, thereby exacerbating cardiac hypoxia and cardiomyocyte death (Figure 3, A–E). Additional treatment with the proangiogenic factor cartilage oligomeric matrix protein–angiopoietin-1 (COMP-Ang1) (17) increased relative vascular density and thereby improved cardiac hypoxia and systolic dysfunction (Supplemental Figure 5, A–C). We also found that a decrease of relative vascular density was associated with cardiac dysfunction, along with upregulation of insulin signaling in spontaneously hypertensive rats (Supplemental Figure 3, A–G), suggesting that cardiac insulin signaling plays a pathological role in HF by increasing a mismatch between cardiomyocyte size and vascularity.

Cardiomyocyte-specific reduction of Insr expression attenuates systolic dysfunction due to pressure overload. To further investigate the role of cardiac insulin signaling, we generated CIRKO mice by using the Cre-loxP system. We prepared transgenic mice in which a transgene encoding Cre recombinase was driven by the cardiomyocyte-specific α-myosin heavy chain (MHC) promoter (18). We then crossed these MHC-Cre mice with mice bearing floxed *Insr* alleles (19) and produced TAC in the resulting mice. Since homozygous CIRKO ($Insr^{flox/flox}$Cre$^+$) mice have been shown to develop systolic dysfunction in response to pressure overload (6), we utilized heterozygous CIRKO ($Insr^{flox/+}$Cre$^+$) mice with reduced cardiac expression of Insr (Figure 4A). These mice had a normal heart size and normal systolic function under physiological conditions (Figure 4, B and C). However, cardiac insulin signaling was markedly attenuated in the TAC heart of CIRKO mice (Figure 4B), and therefore chronic pressure

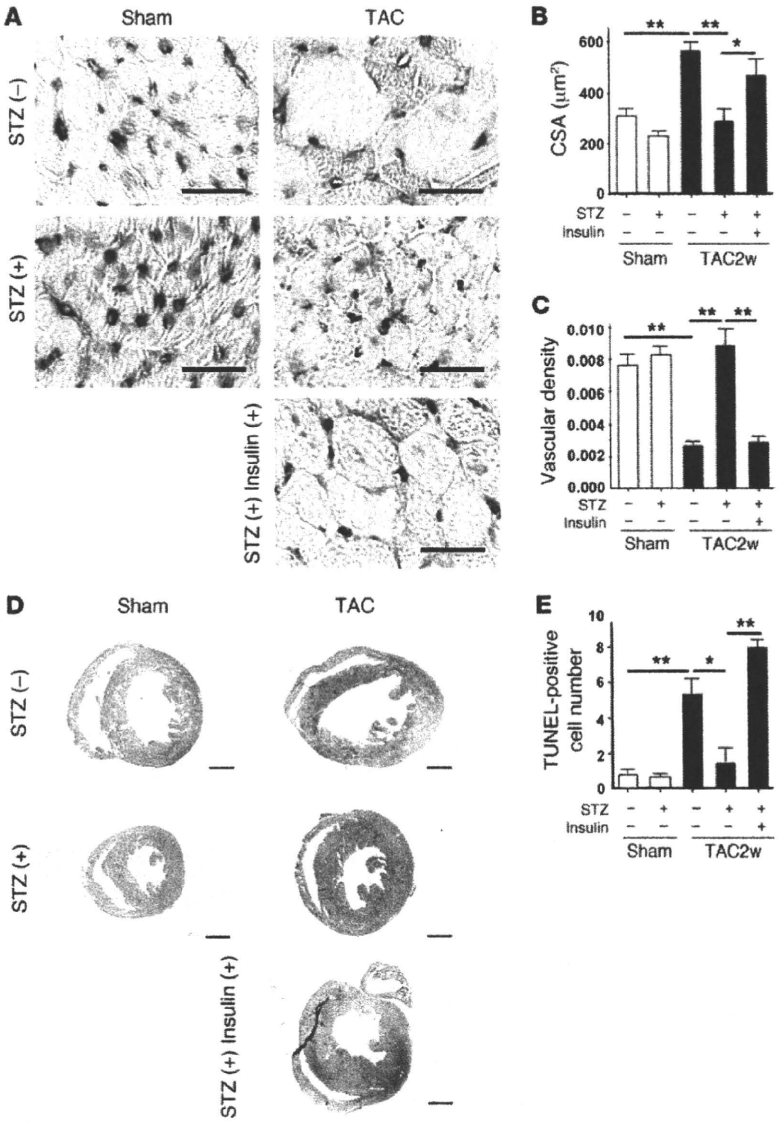

Figure 3

Reduction of plasma insulin inhibits cardiac hypoxia due to pressure overload. (**A**) Animals were prepared as described for Figure 2A. Immunohistochemistry using antibodies against platelet and endothelial cell adhesion molecule (dark brown) and dystrophin (light brown) was performed at 2 weeks after operation. Scale bars: 20 μm. (**B** and **C**) CSA of cardiomyocytes (**B**) and relative vascular density (**C**) were estimated as described in Methods. $n = 4–5$. (**D**) Cardiac ischemia (brown) in mice prepared as described for Figure 2A was estimated with a Hypoxyprobe-1. Scale bars: 1 mm. (**E**) Number of TUNEL-positive cells per 1×10^4 cardiomyocytes. $n = 4–6$. Data are shown as mean ± SEM. $^*P < 0.05$; $^{**}P < 0.01$.

overload caused less severe hypertrophy than in WT mice (Figure 4, C and D). Both systolic dysfunction and left ventricular dilatation were significantly inhibited in CIRKO mice compared with their littermate controls (Figure 4D and Supplemental Figure 6). Histological examination showed that the increase of CSA after TAC was significantly attenuated and relative vascular density was markedly increased in CIRKO mice (Figure 5, A–C). In consequence, the number of dead cardiomyocytes was significantly smaller in CIRKO mice than in their littermate controls (Figure 5D).

To investigate the role of Akt in HF induced by pressure overload, we utilized heterozygous *Akt1*-deficient ($Akt1^{+/-}$) mice. Two weeks after TAC operation, both systolic dysfunction and left ventricular dilatation were significantly inhibited in $Akt1^{+/-}$ mice compared with their littermate controls (Figure 6A). Histological examination showed that the increase of CSA after TAC was significantly attenuated and relative vascular density was markedly increased in $Akt1^{+/-}$ mice (Figure 6, B and C), which was associated with decreased activation of Akt (Figure 6D). These data suggest that sustained activation of Akt could cause cardiac dysfunction under chronic pressure overload.

Mechanism of enhanced cardiac insulin signaling due to pressure overload. To investigate the additional mechanisms by which chronic pressure overload enhances insulin signaling in the heart, we examined pIrs1 levels immediately after TAC. Western blot analysis revealed that pressure overload markedly increased the pIrs1 level from as early as 1 minute after the operation (Figure 7A). Such activation was significantly attenuated in both heterozygous and homozygous CIRKO mice (Figure 7A and Supplemental Figure 7), suggesting that mechanical stress may also upregulate the insulin signaling pathway via direct activation of Insr independent of its ligand. To further investigate the influence of mechanical stress on insulin signaling, we stretched cultured cardiomyocytes by 20% and examined the changes in the pIrs1 level. Consistent with our hypothesis, stretching of cardiomyocytes led to marked activation of insulin sig-

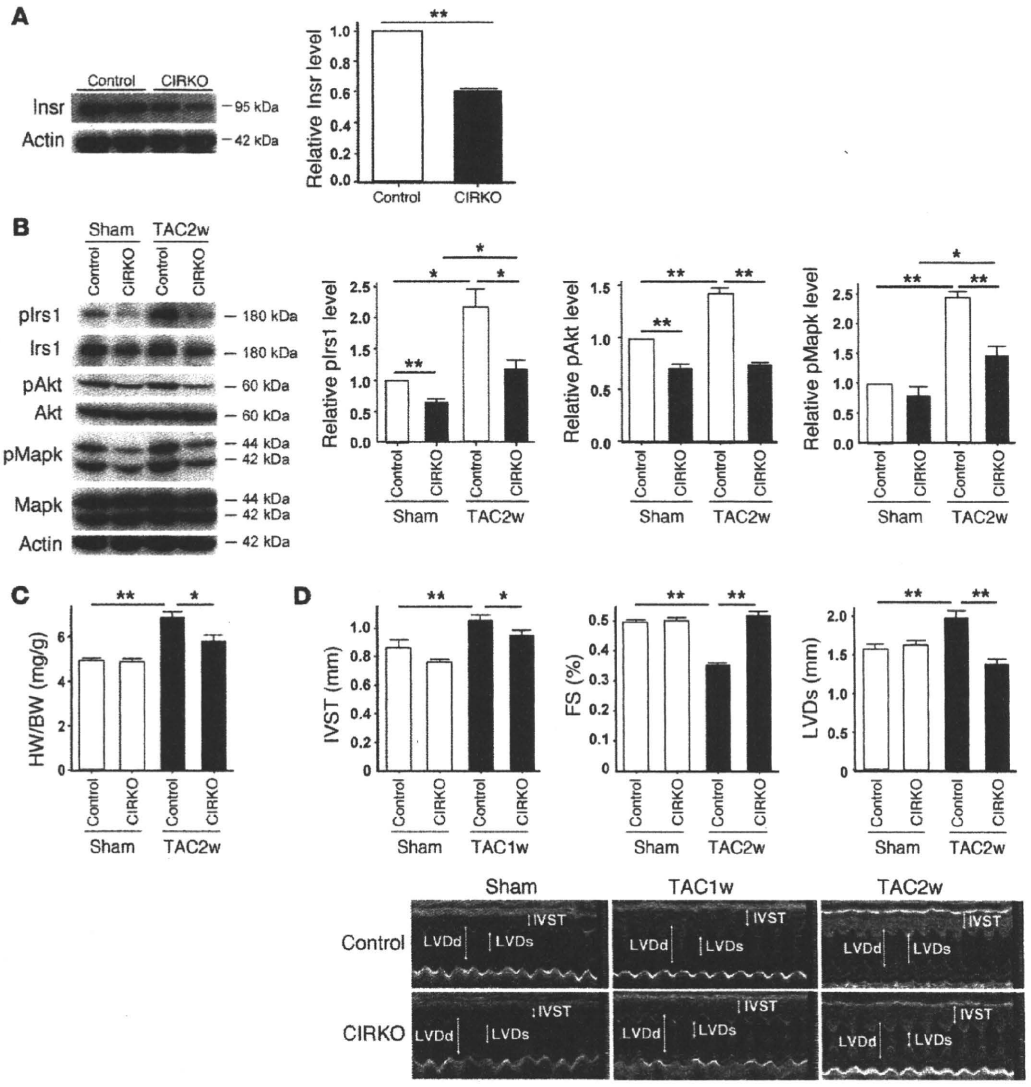

Figure 4

Cardiomyocyte-specific reduction of Insr expression attenuates systolic dysfunction due to pressure overload. (**A**) Western blot analysis of Insr expression in the hearts of CIRKO mice (*Insr*$^{flox/+}$Cre^{+}) and their littermate controls (control). Graphs indicate relative expression levels of Insr. $n = 3$. (**B**) CIRKO mice (*Insr*$^{flox/+}$Cre^{+}) or littermate controls were subjected to TAC or sham operation, and components of the insulin signaling pathway in the heart were examined by Western blot analysis at 2 weeks after operation. Graphs indicate relative expression levels of these signaling molecules. $n = 3$. (**C**) The heart weight/body weight ratio of animals prepared as described in **A** was measured at 2 weeks after operation. $n = 7–9$. (**D**) Cardiac hypertrophy and systolic function of animals prepared as described in **A** were assessed by echocardiography at 1 week (IVST) or 2 weeks (FS and LVDs) after operation. Photographs show representative results of echocardiography (M-mode). $n = 8–13$. Data are shown as mean ± SEM. $^{*}P < 0.05$; $^{**}P < 0.01$.

naling (Figure 7B). This activation was abolished by knockdown of Insr expression (Figure 7C), whereas knockdown of Igf1 or the Igf1 receptor showed a marginal effect (Supplemental Figure 8). These results suggest that mechanical stress mainly enhances insulin signaling through Insr and that Igf1 and the Igf1 receptor contribute to stretch-induced activation of this signaling to a lesser extent. This is similar to the known direct activation of the angiotensin II type I receptor by mechanical stress, which contributes to pathological hypertrophy (20); however, the precise mechanism of how mechanical stress activates insulin signaling needs further investigation.

There is accumulating evidence that suggests a potential relationship between insulin resistance and cardiac hypertrophy (21, 22). Therefore we examined plasma glucose and insulin levels in mice subjected to chronic pressure overload. Both glucose and insulin levels were significantly higher in the TAC group than in the sham-operated group (Figure 7D). More importantly, the homeostasis model assessment–insulin resistance (HOMA-IR) index was markedly elevated in the TAC group (Figure 7D). Furthermore, insulin-induced phosphorylation of Akt was impaired in the liver of the TAC group compared with the sham-operated group (Figure 7E).

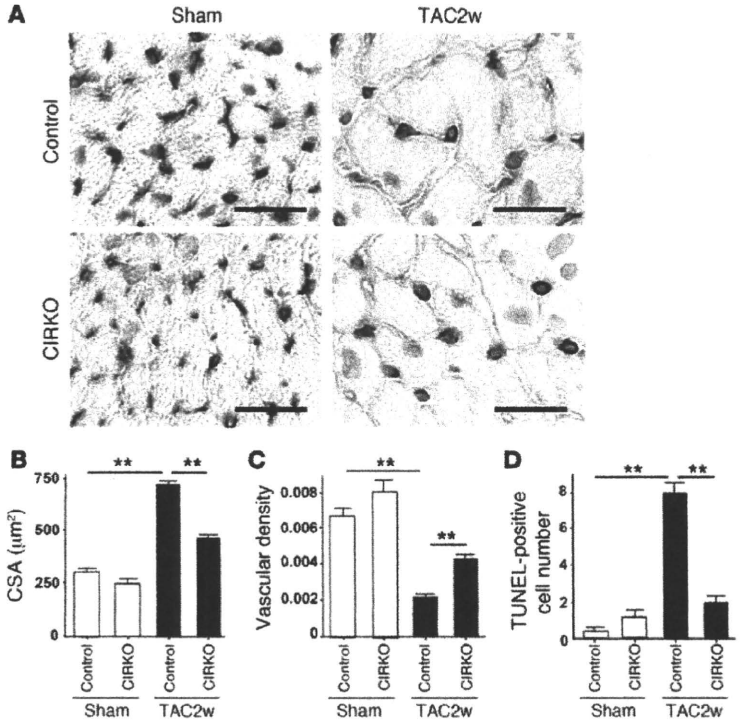

Figure 5
Cardiomyocyte-specific reduction of Insr expression attenuates cardiac hypoxia due to pressure overload. (**A**) CIRKO mice ($Insr^{flox/+}$Cre$^+$) or littermate controls were subjected to TAC or sham operation. Immunohistochemistry using antibodies against platelet and endothelial cell adhesion molecules (dark brown) and dystrophin (light brown) was performed at 2 weeks after operation. Scale bars: 20 μm. (**B** and **C**) CSA of cardiomyocytes (**B**) and relative vascular density (**C**) were estimated as described in Methods. $n = 4–5$. (**D**) Number of TUNEL-positive cells per 1×10^4 cardiomyocytes. $n = 4–5$. Data are shown as mean ± SEM. $^*P < 0.05$; $^{**}P < 0.01$.

These results suggest that chronic pressure overload induces hepatic insulin resistance, thereby inducing hyperinsulinemia, whereas there is no cardiac insulin resistance due to direct activation of Insr as well as to upregulation of Insr and Irs1.

Discussion

A number of clinical studies have strongly indicated the link between insulin resistance and nonischemic HF (23–26). Approximately two-thirds of patients with essential hypertension have abnormal glucose metabolism (27), and there is a positive relationship between cardiac hypertrophy and the plasma insulin concentration (28), suggesting that elevation of insulin contributes to myocardial growth in the presence of chronic pressure overload. Consistent with these reports, we found that chronic pressure overload induced hepatic insulin resistance and increased the plasma insulin level. Myocardial stretch activated Insr, and chronic pressure overload not only increased the activity of insulin signaling (pIrs1 and pAkt levels), but also upregulated the expression of Insr and Irs1 protein. This in turn facilitated activation of cardiac insulin signals by hyperinsulinemia. Such activation enhanced the mismatch between vascularity and cardiomyocyte size and increased cardiomyocyte death. This increase was associated with systolic dysfunction and may be one of the causes of HF induced by chronic pressure overload. However, we have not excluded other mechanisms by which excessive insulin signals promote cardiac dysfunction during pressure overload. For example, cardiac hypoxia may affect metabolism and contraction of myocytes with their viability being unchanged. Indeed, we only showed evidence for tissue hypoxia in the TAC heart by using pimonidazole, which may not be sufficient. We have not demonstrated that inhibition of cardiomyocyte death attenuates systolic dysfunction of the TAC heart. Accordingly, we cannot definitively conclude that hypoxia-induced cardiomyocyte death was essential for the development of HF. It has been reported that endothelial cells in the heart release a variety of factors, such as neuregulin and nitric oxide, that regulate survival and function of cardiomyocytes and that endothelial-myocardial interaction plays a crucial role in maintaining systolic function (29). Thus, it is also possible that a decrease of relative vascular density in the TAC heart impairs such paracrine mechanisms, leading to systolic dysfunction.

Our results were similar to those of the study with conditional Akt transgenic animals (14). In this model, Akt signaling could be switched on or off in the heart. These mice developed physiological hypertrophy following short-term induction, but exhibited pathological hypertrophy with longer periods of Akt activation due to an imbalance between cardiac growth and angiogenesis. Interestingly, cardiac dysfunction was further impaired when Akt was switched off after prolonged activation. These results suggest that Akt signaling itself is beneficial for maintenance of systolic function in this model; however, excessive cardiac growth with insufficient angiogenesis causes pathological hypertrophy. Thus, although insulin/Akt signaling has been implicated in the development of physiological hypertrophy, constitutive activation of these signals can induce HF when coordinated tissue growth and angiogenesis are disrupted.

Alterations of myocardial substrate metabolism have been implicated in the pathogenesis of contractile dysfunction and HF (21, 30). Studies on animal models of HF have demonstrated that, during transition from cardiac hypertrophy to ventricular dysfunction, expression of genes encoding for mitochondrial fatty acid (FA) β-oxidation enzymes shows a coordinated decrease, resulting in a shift of myocardial metabolism that recapitulates the fetal heart gene program, with glucose instead of FA becoming the primary energy substrate (31, 32). Clinical studies have revealed that patients with nonischemic cardiomyopathy exhibit alterations of

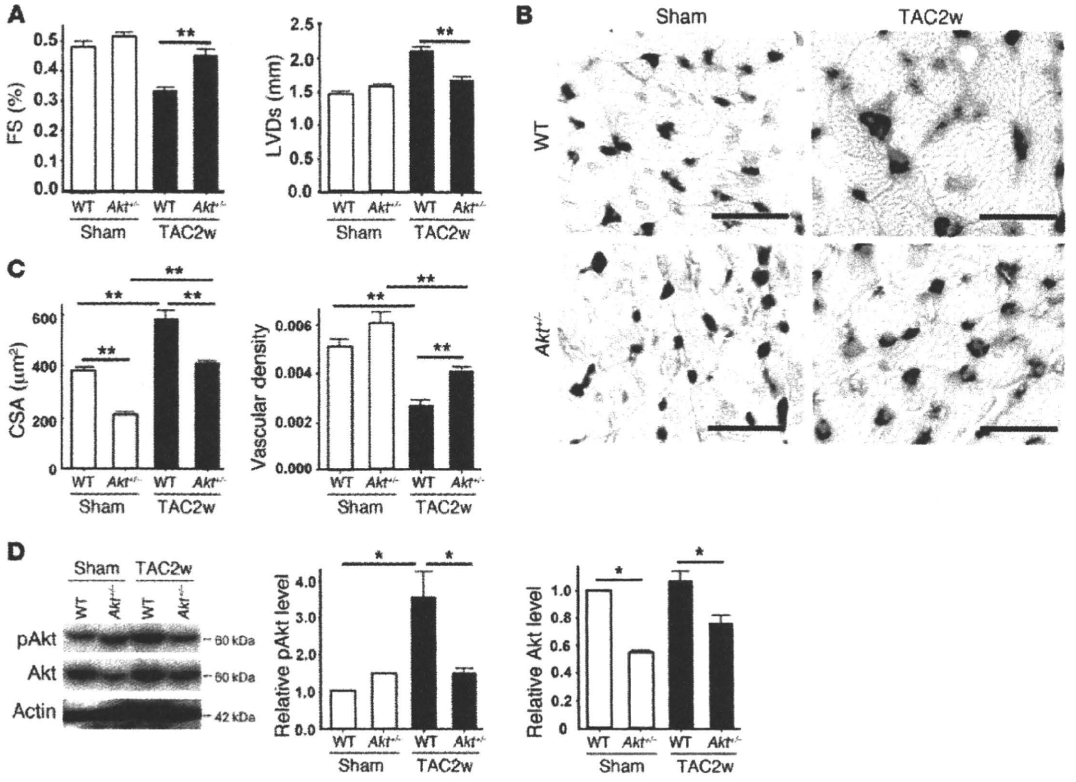

Figure 6

Reduced activation of Akt attenuates systolic dysfunction due to pressure overload. (**A**) *Akt1*-deficient (*Akt1*$^{+/-}$) mice and WT littermates were subjected to TAC or sham operation. Cardiac hypertrophy and systolic function were assessed by echocardiography at 2 weeks after operation. $n = 4$–6. (**B**) Immunohistochemistry using antibodies against platelet and endothelial cell adhesion molecules (dark brown) and dystrophin (light brown) was performed at 2 weeks after operation. Scale bars: 20 μm. (**C**) CSA of cardiomyocytes and relative vascular density were estimated as described in Methods. $n = 3$. (**D**) pAkt and Akt levels in the heart at 2 weeks after operation were examined by Western blot analysis. Graphs indicate relative expression levels of pAkt and Akt. $n = 3$. Data are shown as mean ± SEM. $^*P < 0.05$; $^{**}P < 0.01$.

myocardial metabolism that are characterized by a decrease of FA metabolism and an increase of myocardial glucose metabolism, a pattern similar to that shown in animal models of HF (33). Under these conditions, increased FA metabolism in the heart is pathogenic and the extent of abnormal FA metabolism predicts both morphologic changes of the heart and a poor clinical outcome (34). In this respect, activation of the insulin/Akt pathway in the failing heart appears to be an adaptive response, but constitutive activation of this pathway also leads to activation of growth signals that results in dysregulated hypertrophy, cardiac hypoxia, and systolic dysfunction. Thus, a metabolic modulator that increases glucose uptake (or decreases FA metabolism) without activation of insulin signaling would be a better strategy for the treatment of HF because these patients have systemic insulin resistance. Our results also suggest that the use of insulin to control hyperglycemia can be harmful, especially in the setting of pressure overload, a finding that is consistent with the outcome of a recent clinical trial (16).

Multiple counterregulatory hormones and cytokines are upregulated in HF and are likely to play a role in insulin resistance and altered glucose disposition (21). Upregulation of catecholamines not only contributes directly to the pathogenesis of cardiomyopathy but also increases insulin resistance and thereby indirectly affects systolic function. We also found that chronic pressure overload increased the production of proinflammatory cytokines by adipose tissue, thus promoting systemic insulin resistance (I. Shimizu and T. Minamino, unpublished observations). Further investigation of the link between insulin resistance and HF will continue to provide novel insights into the treatment of HF.

Methods

Animal models. All animal study protocols were approved by the Chiba University Review Board. C57BL/6 mice were purchased from SLC Japan. TAC was performed as described previously (15) in 11-week-old male mice. Sham-operated mice underwent the same procedure except for aortic constriction. For the type 1 diabetic model, 7-week-old male C57BL/6 mice were treated with i.p. STZ in 0.1 M sodium citrate (pH 4.5) at a dose of 50 mg/kg for 5 days. TAC was performed 4 weeks after STZ treatment. In the insulin-treated group, mice received daily i.p. injection of insulin (0.1 IU/g/d) from 9 weeks (2 weeks after STZ treatment) to 13 weeks of age (2 weeks after TAC). In some experiments, mice received an i.p. injection of insulin (1 IU/kg) 30 minutes before sacrifice to investigate the insulin sensitivity of various organs. *Akt1*-deficient mice (*Akt1*$^{+/-}$) were a gift from Morris J. Birnbaum (University of Pennsylvania School of Medicine, Philadelphia, Pennsylvania, USA). The generation and genotyping of *Akt1*-deficient mice, floxed *Insr* mice, and MHC-Cre mice have been described previously (18, 19, 35). Littermate controls have the genotype *Insr*$^{flox/+}$ or *Insr*$^{flax/flox}$. We

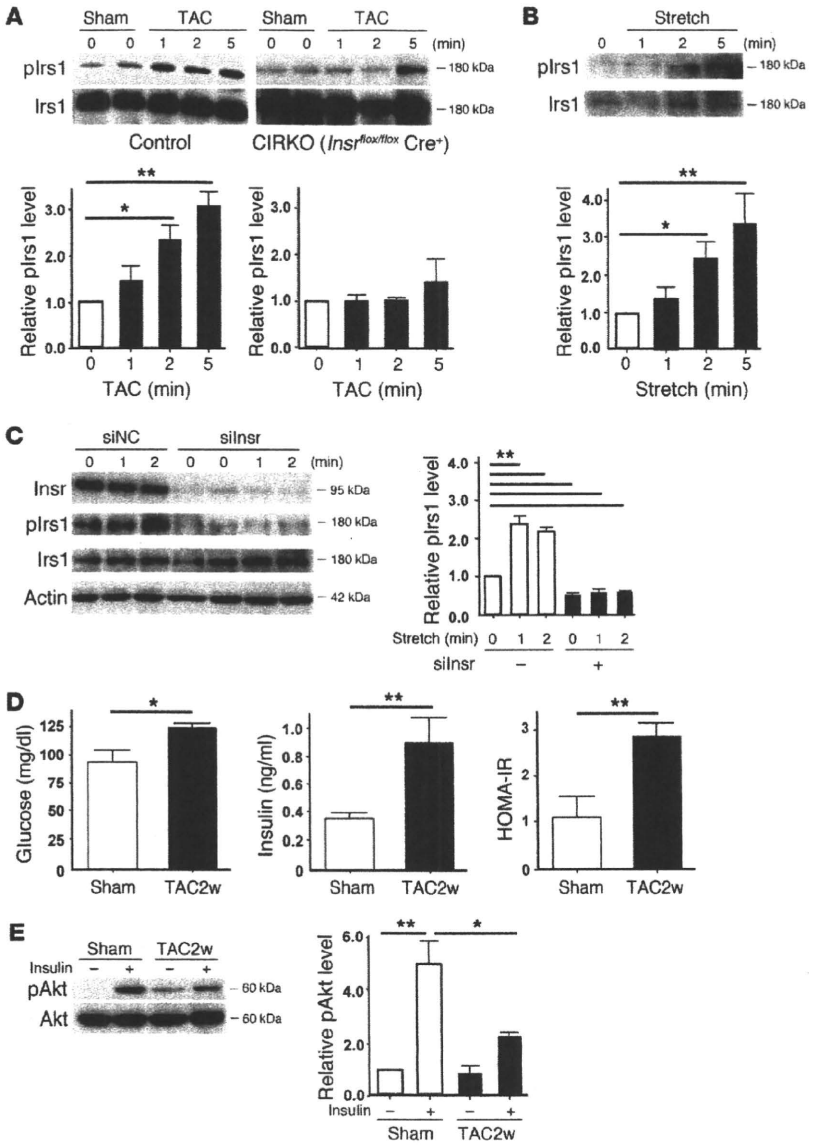

Figure 7
Mechanism of enhanced insulin signaling in the heart during pressure overload. (**A**) CIRKO mice (*Insr*$^{flox/flox}$Cre^{+}) or littermate controls were subjected to TAC or sham operation, and heart samples were obtained at the indicated times. pIrs1 levels were examined by Western blot analysis. The graphs indicate relative expression levels of pIrs1. $n = 3$. (**B**) Cardiomyocytes were subjected to mechanical stretch and pIrs1 levels were examined by Western blot analysis. $n = 3$. (**C**) siRNA targeting Insr (siInsr) or negative control RNA (siNC) was introduced into cardiomyocytes, after which the cells were subjected to mechanical stretch. pIrs1 levels were examined by Western blot analysis. $n = 3$. (**D**) Plasma glucose and insulin levels were examined at 2 weeks after TAC. $n = 7$–8. (**E**) Insulin-induced phosphorylation of Akt (pAkt) in the liver was examined after TAC or sham operation. $n = 3$. Data are shown as mean ± SEM. $^{*}P < 0.05$; $^{**}P < 0.01$.

administered adenoviral vector encoding COMP-Ang1 to mice i.v. after TAC operation as previously described (17).

Physiological and histological analyses. Echocardiography was performed with a Vevo 770 High Resolution Imaging System (Visual Sonics Inc.). To minimize variation of the data, the heart rate was always approximately 500–600 beats per minute when cardiac function was assessed. Cardiac tissue was fixed by perfusion with 4% paraformaldehyde. The fixed sample was immersed in OCT compounds (Miles Inc.) and snap-frozen in liquid nitrogen to prepare cryostat sections. Frozen cross sections of hearts were immunohistochemically double stained with antibodies for PECAM (BD Biosciences – Pharmingen) and dystrophin (Novocastra Laboratories). For measurement of the CSA of cardiomyocytes, 50 randomly selected cardiomyocytes in a left ventricular cross section were measured by tracing dystrophin immunostaining with NIH ImageJ software (http://rsbweb.nih.gov/ij/). Using the same sections, the number of PECAM-positive vessels was counted, and vascular density was estimated as the number of microvessels/number of cardiomyocytes/CSA. Tissue hypoxia was estimated with the Hypoxyprobe-1 (Chemicon) according to the manufacturer's instructions. Briefly, an i.p. injection of pimonidazole (60 mg/kg) was performed 90 minutes before sacrifice. Heart samples were harvested and fixed in 10% formalin overnight. The samples were embedded in paraffin, sectioned at 4-μm thickness, and stained with the Hypoxyprobe-1 monoclonal antibody (clone 4.3.11.3), which binds to protein adducts of pimonidazole in hypoxic cells. TUNEL labeling was performed according to the manufacturer's protocol (In Situ Apoptosis Detection Kit; TaKaRa) in combination with immunostaining for appropriate cell markers.

Western blot analysis. Whole-cell lysates were prepared in lysis buffer (10 mM Tris-HCl, pH 8, 140 mM NaCl, 5 mM EDTA, 0.025% NaN3, 1% Triton X-100, 1% deoxycholate, 0.1% SDS, 1 mM PMSF, 5 μg/ml leupeptin, 2 μg/ml aprotinin, 50 mM NaF, and 1 mM Na_2VO_3). The lysates (40–50 μg) were resolved by SDS-PAGE. Proteins were transferred to a PVDF membrane (Millipore), which was incubated with the primary antibody followed by anti-rabbit or anti-mouse immunoglobulin-G conjugated with horseradish peroxidase (Jackson). Specific proteins were detected by enhanced chemiluminescence

(Amersham). The primary antibodies used for Western blotting were as follows: anti-pIrs1 antibody (Tyr612, Biomol), anti-Irs1 antibody (C20), anti-Akt1 antibody (C20), anti-Insr β antibody (C-19) (Santa Cruz Biotechnology Inc.), anti-phospho-Akt antibody (Ser473), anti-phospho-p44/42 MAP kinase antibody (Thr202/Tyr204), anti-MAP kinase (ERK1+ERK2) antibody (Invitrogen), and anti-actin antibody (Sigma-Aldrich). Plasma insulin levels were evaluated with an ELISA kit (Morinaga Institute of Biological Science Inc.) according to the manufacturer's instructions.

Cell culture. Neonatal Wistar rats were purchased from Takasugi Experimental Animal Supply. Cardiomyocytes were prepared from neonatal rats and cultured as described previously (15). Passive stretching of cultured cells was done as described previously. Cells were plated on collagen-coated silicone rubber dishes (STREX Mechanical Cell Strain Instruments), and the silicone dishes were stretched by attaching both ends of each dish firmly to a fixed frame, resulting in longitudinal stretch by 20% of the original length. siRNA targeting Insr, IGF, and the IGF-1 receptor was purchased from Invitrogen and introduced into rat cardiomyocytes by using Lipofectamine RNAiMax (Invitrogen) according to the manufacturer's instructions.

Statistics. Data are shown as the mean ± SEM. Differences between groups were examined by 2-tailed Student's *t* test or ANOVA, followed by Bonferroni's correction for comparison of means. For all analyses, $P < 0.05$ was considered statistically significant.

Acknowledgments

We thank Morris J. Birnbaum for *Akt1*-deficient mice. This work was supported by a Grant-in-Aid for Scientific Research from the Ministry of Education, Science, Sports, and Culture and Health and Labor Sciences research grants (to I. Komuro); a Grant-in-Aid for Scientific Research from the Ministry of Education, Culture, Sports, Science and Technology of Japan; and grants from the Suzuken Memorial Foundation; the Japan Diabetes Foundation; the Ichiro Kanehara Foundation; the Tokyo Biochemical Research Foundation; the Takeda Science Foundation; the Cell Science Research Foundation; the Japan Foundation of Applied Enzymology; and the Astellas Foundation for Research on Metabolic Disorders (to T. Minamino).

Received for publication June 5, 2009, and accepted in revised form February 10, 2010.

Address correspondence to: Issei Komuro, Department of Cardiovascular Science and Medicine, Chiba University Graduate School of Medicine, 1-8-1 Inohana, Chuo-ku, Chiba 260-8670, Japan. Phone: 81.43.226.2097; Fax: 81.43.226.2557; E-mail: komuro-tky@umin.ac.jp.

1. Frey N, Olson EN. Cardiac hypertrophy: the good, the bad, and the ugly. *Annu Rev Physiol.* 2003;65:45–79.
2. Adams TD, Yanowitz FG, Fisher AG, Ridges JD, Lovell K, Pryor TA. Noninvasive evaluation of exercise training in college-age men. *Circulation.* 1981; 64(5):958–965.
3. Pelliccia A, Maron BJ. Outer limits of the athlete's heart, the effect of gender, and relevance to the differential diagnosis with primary cardiac diseases. *Cardiol Clin.* 1997;15(3):381–396.
4. Heineke J, Molkentin JD. Regulation of cardiac hypertrophy by intracellular signalling pathways. *Nat Rev Mol Cell Biol.* 2006;7(8):589–600.
5. Belke DD, et al. Insulin signaling coordinately regulates cardiac size, metabolism, and contractile protein isoform expression. *J Clin Invest.* 2002; 109(5):629–639.
6. Hu P, Zhang D, Swenson L, Chakrabarti G, Abel ED, Litwin SE. Minimally invasive aortic banding in mice: effects of altered cardiomyocyte insulin signaling during pressure overload. *Am J Physiol Heart Circ Physiol.* 2003;285(3):H1261–H1269.
7. Shioi T, et al. The conserved phosphoinositide 3-kinase pathway determines heart size in mice. *EMBO J.* 2000;19(11):2537–2548.
8. McMullen JR, et al. Phosphoinositide 3-kinase (p110α) plays a critical role for the induction of physiological, but not pathological, cardiac hypertrophy. *Proc Natl Acad Sci U S A.* 2003;100(21):12355–12360.
9. DeBosch B, et al. Akt1 is required for physiological cardiac growth. *Circulation.* 2006;113(17):2097–2104.
10. Samuelsson AM, et al. Hyperinsulinemia: effect on cardiac mass/function, angiotensin II receptor expression, and insulin signaling pathways. *Am J Physiol Heart Circ Physiol.* 2006;291(2):H787–H796.
11. Condorelli G, et al. Akt induces enhanced myocardial contractility and cell size in vivo in transgenic mice. *Proc Natl Acad Sci U S A.* 2002;99(19):12333–12338.
12. Matsui T, et al. Phenotypic spectrum caused by transgenic overexpression of activated Akt in the heart. *J Biol Chem.* 2002;277(25):22896–22901.
13. Shioi T, et al. Akt/protein kinase B promotes organ growth in transgenic mice. *Mol Cell Biol.* 2002; 22(8):2799–2809.
14. Shiojima I, et al. Disruption of coordinated cardiac hypertrophy and angiogenesis contributes to the transition to heart failure. *J Clin Invest.* 2005; 115(8):2108–2118.
15. Sano M, et al. p53-induced inhibition of Hif-1 causes cardiac dysfunction during pressure overload. *Nature.* 2007;446(7134):444–448.
16. Gerstein HC, et al. Effects of intensive glucose lowering in type 2 diabetes. *N Engl J Med.* 2008; 358(24):2545–2559.
17. Cho CH, et al. Long-term and sustained COMP-Ang1 induces long-lasting vascular enlargement and enhanced blood flow. *Circ Res.* 2005;97(1):86–94.
18. Abel ED, et al. Cardiac hypertrophy with preserved contractile function after selective deletion of GLUT4 from the heart. *J Clin Invest.* 1999;104(12):1703–1714.
19. Bruning JC, et al. A muscle-specific insulin receptor knockout exhibits features of the metabolic syndrome of NIDDM without altering glucose tolerance. *Mol Cell.* 1998;2(5):559–569.
20. Zou Y, et al. Mechanical stress activates angiotensin II type 1 receptor without the involvement of angiotensin II. *Nat Cell Biol.* 2004;6(6):499–506.
21. Witteles RM, Fowler MB. Insulin-resistant cardiomyopathy clinical evidence, mechanisms, and treatment options. *J Am Coll Cardiol.* 2008;51(2):93–102.
22. Sharma N, Okere IC, Duda MK, Chess DJ, O'Shea KM, Stanley WC. Potential impact of carbohydrate and fat intake on pathological left ventricular hypertrophy. *Cardiovasc Res.* 2007;73(2):257–268.
23. Swan JW, et al. Insulin resistance in chronic heart failure: relation to severity and etiology of heart failure. *J Am Coll Cardiol.* 1997;30(2):527–532.
24. Ingelsson E, Sundstrom J, Arnlov J, Zethelius B, Lind L. Insulin resistance and risk of congestive heart failure. *JAMA.* 2005;294(3):334–341.
25. Arnlov J, et al. Several factors associated with the insulin resistance syndrome are predictors of left ventricular systolic dysfunction in a male population after 20 years of follow-up. *Am Heart J.* 2001; 142(4):720–724.
26. Hasegawa S, Kusuoka H, Maruyama K, Nishimura T, Hori M, Hatazawa J. Myocardial positron emission computed tomographic images obtained with fluorine-18 fluoro-2-deoxyglucose predict the response of idiopathic dilated cardiomyopathy patients to beta-blockers. *J Am Coll Cardiol.* 2004; 43(2):224–233.
27. Garcia-Puig J, Ruilope LM, Luque M, Fernandez J, Ortega R, Dal-Re R. Glucose metabolism in patients with essential hypertension. *Am J Med.* 2006; 119(4):318–326.
28. Karason K, Sjostrom L, Wallentin I, Peltonen M. Impact of blood pressure and insulin on the relationship between body fat and left ventricular structure. *Eur Heart J.* 2003;24(16):1500–1505.
29. Brutsaert DL. Cardiac endothelial-myocardial signaling: its role in cardiac growth, contractile performance, and rhythmicity. *Physiol Rev.* 2003;83(1):59–115.
30. Neubauer S. The failing heart--an engine out of fuel. *N Engl J Med.* 2007;356(11):1140–1151.
31. Christe ME, Rodgers RL. Altered glucose and fatty acid oxidation in hearts of the spontaneously hypertensive rat. *J Mol Cell Cardiol.* 1994;26(10):1371–1375.
32. Barger PM, Kelly DP. Fatty acid utilization in the hypertrophied and failing heart: molecular regulatory mechanisms. *Am J Med Sci.* 1999;318(1):36–42.
33. Davila-Roman VG, et al. Altered myocardial fatty acid and glucose metabolism in idiopathic dilated cardiomyopathy. *J Am Coll Cardiol.* 2002;40(2):271–277.
34. Yazaki Y, et al. Assessment of myocardial fatty acid metabolic abnormalities in patients with idiopathic dilated cardiomyopathy using 123I BMIPP SPECT: correlation with clinicopathological findings and clinical course. *Heart.* 1999;81(2):153–159.
35. Cho H, Thorvaldsen JL, Chu Q, Feng F, Birnbaum MJ. Akt1/PKBalpha is required for normal growth but dispensable for maintenance of glucose homeostasis in mice. *J Biol Chem.* 2001;276(42):38349–38352.

Promotion of CHIP-Mediated p53 Degradation Protects the Heart From Ischemic Injury

Atsuhiko T. Naito, Sho Okada, Tohru Minamino, Koji Iwanaga, Mei-Lan Liu, Tomokazu Sumida, Seitaro Nomura, Naruhiko Sahara, Tatsuya Mizoroki, Akihiko Takashima, Hiroshi Akazawa, Toshio Nagai, Ichiro Shiojima, Issei Komuro

Rationale: The number of patients with coronary heart disease, including myocardial infarction, is increasing and novel therapeutic strategy is awaited. Tumor suppressor protein p53 accumulates in the myocardium after myocardial infarction, causes apoptosis of cardiomyocytes, and plays an important role in the progression into heart failure.

Objectives: We investigated the molecular mechanisms of p53 accumulation in the heart after myocardial infarction and tested whether anti-p53 approach would be effective against myocardial infarction.

Methods and Results: Through expression screening, we found that CHIP (carboxyl terminus of Hsp70-interacting protein) is an endogenous p53 antagonist in the heart. CHIP suppressed p53 level by ubiquitinating and inducing proteasomal degradation. CHIP transcription was downregulated after hypoxic stress and restoration of CHIP protein level prevented p53 accumulation after hypoxic stress. CHIP overexpression in vivo prevented p53 accumulation and cardiomyocyte apoptosis after myocardial infarction. Promotion of CHIP function by heat shock protein (Hsp)90 inhibitor, 17-allylamino-17-demethoxy geldanamycin (17-AAG), also prevented p53 accumulation and cardiomyocyte apoptosis both in vitro and in vivo. CHIP-mediated p53 degradation was at least one of the cardioprotective effects of 17-AAG.

Conclusions: We found that downregulation of CHIP level by hypoxia was responsible for p53 accumulation in the heart after myocardial infarction. Decreasing the amount of p53 prevented myocardial apoptosis and ameliorated ventricular remodeling after myocardial infarction. We conclude that anti-p53 approach would be effective to treat myocardial infarction. (*Circ Res*. 2010;106:1692-1702.)

Key Words: myocardial infarction ■ CHIP ■ p53 ■ hypoxia

The number of patients with coronary heart disease has been increasing and cardiovascular diseases are the leading cause of deaths in the Western world. Despite the development of pharmacological and nonpharmacological interventions, 33% of the men and 43% of the women die within 5 years after myocardial infarction (MI).[1] Therefore, a novel therapeutic approach against coronary heart disease is awaited.

Apoptosis of cardiomyocytes is accompanied with acute coronary occlusion.[2] Because apoptotic loss of cardiomyocytes causes heart failure,[3] inhibition of apoptosis has been suggested as an additional therapeutic approach to coronary heart disease.[4] In mice, overexpression of antiapoptotic Bcl-2 protein or genetic deletion of proapoptotic Bax protein have been reported to prevent apoptosis and reduce infarct size,[5–8] implicating that antiapoptotic approach is effective for prevention of ventricular remodeling after myocardial infarction.

The tumor suppressor *p53* is an important transcription factor that regulates cell cycle progression, cellular senescence, and apoptosis. Under physiological condition, p53 protein level is maintained low, but is elevated when cells are stressed or damaged.[9] The mechanism for keeping p53 protein level low involves several E3 ubiquitin ligases such as MDM2,[10,11] COP1,[12] and Pirh2.[13] Importantly, the expression of these proteins were positively regulated by p53, suggesting the role for negative-feedback loop against p53 elevation.

Protein level of p53 is also kept low in the heart but it is elevated when cardiac cells are exposed to hypoxia.[14–16]

Original received December 4, 2009; revision received April 6, 2010; accepted April 12, 2010.

From the Department of Cardiovascular Science and Medicine (A.T.N., S.O., T. Minamino, K.I., M.-L.L., T.S., S.N., H.A., T.N., I.S., I.K.), Chiba University Graduate School of Medicine, Japan; Department of Cardiovascular Medicine (A.T.N., H.A., I.S., I.K.), Osaka University Graduate School of Medicine, Japan; PRESTO (T. Minamino), Japan Science and Technology Agency, Saitama, Japan; and Laboratory for Alzheimer's Disease (N.S., T. Mizoroki, A.T.). RIKEN Brain Science Institute, Saitama, Japan.

This manuscript was sent to Junichi Sadoshima, Consulting Editor, for review by expert referees, editorial decision, and final disposition.

Correspondence to Issei Komuro, MD, PhD, Department of Cardiovascular Science and Medicine, Chiba University Graduate School of Medicine, 1-8-1 Inohana, Chuo-ku, Chiba, Japan. E-mail komuro-tky@umin.ac.jp

Circulation Research **is available at http://circres.ahajournals.org** **DOI: 10.1161/CIRCRESAHA.109.214346**

We have recently reported that elevation of p53 causes the development of pressure overload-induced heart failure.[16] We have also observed the elevation of p53 protein levels after myocardial infarction and shown that *p53* gene deletion improved cardiac function after myocardial infarction,[16] suggesting that the inhibition of p53 might become a novel therapeutic strategy for ischemic heart diseases.

As an initial approach for the investigation of anti-p53 therapy, we searched for an endogenous p53 antagonist in the heart. Through expression screening, we found that CHIP (carboxyl terminus of Hsp70-interacting protein) is an endogenous p53 antagonist that keeps p53 level low in the heart. We also found that CHIP downregulation is involved in the mechanism of p53 accumulation in the heart after myocardial infarction. Facilitating CHIP-mediated p53 degradation prevented apoptosis of cardiomyocytes and ameliorated ventricular remodeling in the postinfarct heart. The present study revealed the mechanism of p53 accumulation in the heart after myocardial ischemia and suggested that anti-p53 approach would be effective to treat myocardial infarction.

Non-standard Abbreviations and Acronyms

17-AAG	17-allylamino-17-demethoxy geldanamycin
CHIP	carboxyl terminus of Hsp70-interacting protein
HIF	hypoxia-inducible factor
HRE	hypoxia-responsive element
Hsp	heat shock protein
HW/BW	heart weight/body weight
MI	myocardial infarction
PARP	poly(ADP-ribose)polymerase
siRNA	small interfering RNA

Methods

Expression Cloning

Expression cloning was performed as described previously[17] using PG13-Luc (kind gift from B. Vogelstein, Ludwig Center for Cancer Genetics and Therapeutics, Howard Hughes Medical Institute, and Sidney Kimmel Cancer Center, Johns Hopkins Medical Institutions, Baltimore, Md) as a reporter plasmid. Initially, cDNA expression library from human heart (Invitrogen) was separated into small pools that contain ≈100 clones each. cDNA clones that downregulate PG13 activity were isolated by sib-selection.

Cell Culture

COS7 and HEK293 cells are from ATCC and cultured in DMEM containing 10% FBS (Invitrogen). Neonatal rat cardiomyocytes were isolated from 1-day-old Wistar rats and cultured as described previously.[18] Cardiomyocytes were exposed to hypoxic stress by culturing under $CoCl_2$ or by culturing in hypoxic chamber (<1% O_2; Po_2, 18 to ≈20 mm Hg).

Animals

All protocols were approved by Chiba University review board. CHIP knockout mice and cardiac-specific inducible hypoxia-inducible factor (HIF)-1 knockout mice were described.[16,19,20] Heterozygous CHIP knockout mice were used in this study because homozygous knockout mice were perinatally lethal.[20] Cardiac-specific CHIP transgenic mice were generated by pronuclear injection of αMHC-HA-CHIP transgene construct. Coronary artery ligation was performed on 10-week old male mice as described previously.[21]

Statistical Analysis

Data are expressed as means±SE. The significance of differences among means was evaluated using analysis of variance (ANOVA), followed by Fisher's protected least significant difference test and Dunnett's test for multiple comparisons. Significant differences were defined as $P<0.05$.

Results

Identification of CHIP As a Novel p53 Antagonist From Heart cDNA Library

To elucidate novel p53 antagonists in the heart, we performed expression screening by expressing cDNA pools in COS7 cells together with a reporter plasmid, PG13-luciferase, which contains 13 copies of p53 binding site upstream of luciferase gene and responsive to wild-type p53 dependent transcription. From the screening of 500 cDNA pools, each containing around 100 individual cDNA clones obtained from human heart cDNA library, we found 5 pools that suppress the PG13 activity. Individual cDNA clone that downregulates the PG13 activity was identified by sib-selection. One of the molecules that was highly expressed in the heart (Figure I, A, in the Online Data Supplement, available at http://circres.ahajournals.org) was CHIP (also called STUB1 [Stip1 homology and U-box containing protein]), a chaperone-interacting protein with E3 ubiquitin ligase activity.[22] Transfection of CHIP suppressed endogenous and exogenous (by overexpression of p53) PG13 activity (Figure 1A) and decreased the protein levels of p53 (Figure 1B) in a plasmid dose-dependent manner in COS7 cells. Direct interaction between CHIP and p53 was confirmed both at the exogenous level in COS7 cells (Online Figure I, B) and at the endogenous level in cardiomyocytes (Online Figure I, C). Western blotting using anti-ubiquitin antibody after immunoprecipitation with p53 revealed that overexpression of CHIP increased poly-ubiquitinated p53 (which appears as a smear) (Online Figure I, D). The proteasomal inhibitor MG132 restored p53 protein level that was suppressed by CHIP (Online Figure I, E), indicating that CHIP directs p53 for proteasome-mediated degradation. When CHIP was knocked down in cardiomyocytes using small interfering (si)RNA, p53 expression was upregulated (Figure 1C), and p53 protein levels following CHIP knockdown were comparable to those induced by the knockdown of MDM2, a well known E3 ubiquitin ligase for p53 (Figure 1D). CHIP protein level was not changed by knockdown of MDM2 (Figure 1D). p53 protein levels were also markedly elevated in the heart of CHIP heterozygous mice (Figure 1E). These results suggest that CHIP induces degradation of wild-type p53 protein in cardiomyocytes, which is consistent with previous reports in other cells (H1299 cells and U2OS cells).[23,24] In addition, we revealed that CHIP is a crucial negative regulator that keeps p53 protein levels low in the heart under physiological conditions.

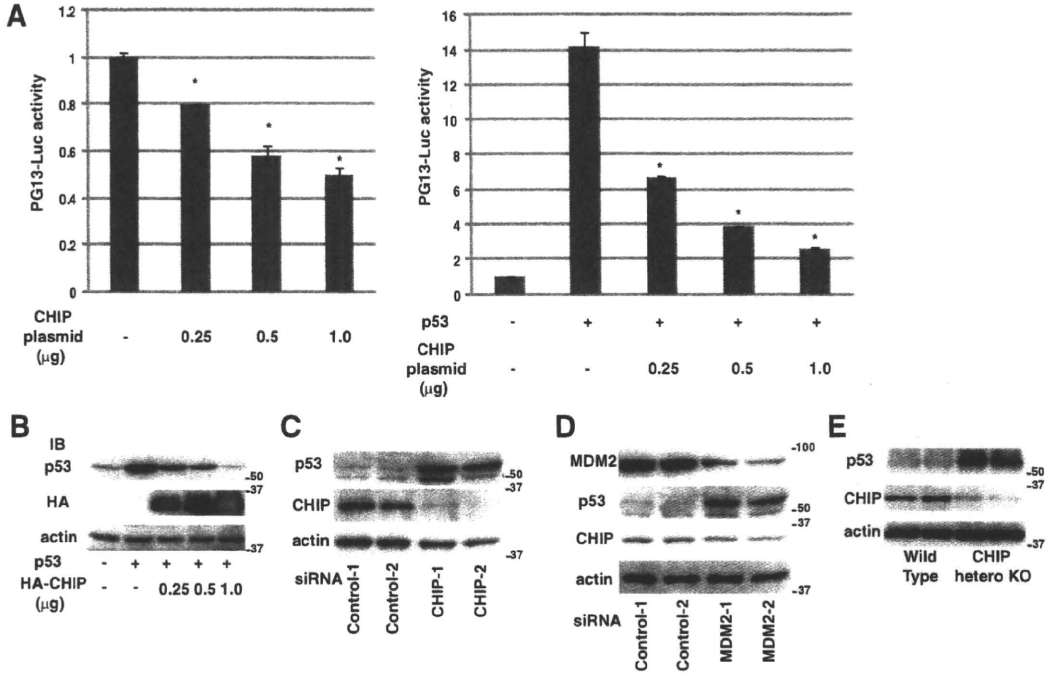

Figure 1. CHIP is a crucial negative regulator of p53 expression in the heart. A, Transfection of CHIP expressing plasmid suppressed endogenous **(left)** and exogenous **(right)** p53 transcriptional activity. *$P<0.01$ vs control; n=5. **B,** CHIP decreases p53 protein levels in COS7 cells. IB indicates immunoblot. **C,** p53 expression is upregulated by CHIP knockdown in cardiomyocytes. siRNAs specific to CHIP (CHIP-1 and CHIP-2), or control siRNA were transfected into cultured cardiomyocytes and protein levels of CHIP and p53 were examined by Western blotting. CHIP-1 and CHIP-2 represent 2 different siRNAs against CHIP. Control-1 is a commercially available control RNA, and control-2 is a scrambled control RNA. **D,** p53 upregulation is also observed by MDM2 knockdown. siRNAs specific to MDM2 (MDM2–1 and MDM2–2) or control siRNA were transfected into cultured cardiomyocytes, and protein levels of CHIP, p53, and MDM2 were examined by Western blotting. The extent of p53 upregulation by MDM2 knockdown was comparable to that induced by CHIP knockdown. **E,** Total protein of wild-type and CHIP heterozygous mice were analyzed by Western blotting. p53 expression is upregulated in the heart of CHIP heterozygous mice.

Molecular Mechanisms of Hypoxia-Induced p53 Accumulation

As CHIP regulates p53 status in the heart, we speculated that CHIP might be involved in the molecular mechanism of hypoxia-induced p53 accumulation in the heart. Cobalt chloride ($CoCl_2$) increases HIF-1 activity through preventing HIF-1α protein degradation and is widely used as a hypoxia mimicking reagent.[25,26] Treatment of cardiomyocytes with $CoCl_2$ (250 μmol/L) increased p53 protein level with a marked downregulation of CHIP protein level (Figure 2A). Notably, the expression of MDM2 was rather increased in this experimental condition. Because transcriptional regulation of MDM2 is known to be upregulated by p53 as a part of negative-feedback loop, increased MDM2 expression after $CoCl_2$ treatment may possibly be attributable to this feedback system against p53 elevation. Accumulation of p53 and downregulation of CHIP were also observed when cardiomyocytes were cultured in hypoxic chamber for 24 hours (Online Figure I, F). We confirmed that both treatments increased nuclear HIF-1α protein that binds to HIF-1α binding oligonucleotide by commercially available ELISA system (Online Figure I, G). We also analyzed the expression of p53 and CHIP in the heart after MI. p53 protein levels were increased on day 1 after MI and remained upregulated thereafter, whereas expression levels of CHIP were markedly downregulated on day 1, and remained at lower levels than those of controls (Figure 2B and analyzed in Online Figure II, A and B). In contrast, MDM2 protein levels were slightly increased after MI (Figure 2B). The inverse correlation between CHIP and p53 protein level implies the possible involvement of CHIP downregulation in the initiation of p53 accumulation after acute hypoxic stress. Other E3 ubiquitin ligases whose transcription is regulated by p53, such as MDM2, might work to reverse p53 level after initial accumulation of p53 as a feedback system to prevent further detrimental effects that might be elicited by chronic p53 elevation.

To investigate why CHIP is downregulated after hypoxic insult, we tested whether HIF-1 mediates hypoxia-induced downregulation of CHIP, because HIF-1 is known to downregulate some of its target genes through hypoxia-responsive element (HRE).[27–30] Human CHIP promoter (from −329 bases upstream of transcription start site to +39 bases downstream of transcription start site) that contains a conserved HRE at −49 (Figure 2C) was cloned upstream of luciferase reporter gene (pGL4-CHIP). pGL4-CHIP activity was significantly suppressed by both $CoCl_2$ treatment (24 hours) and HIF-1α overexpression in COS7 cells (Figure 2D). When a mutation was introduced into HRE at −49 (pGL4-CHIP-mutHRE), the luciferase activity was no longer responsive to hypoxic stress or HIF-1α overexpression (Figure 2D), suggesting that *CHIP* gene expression is downregu-

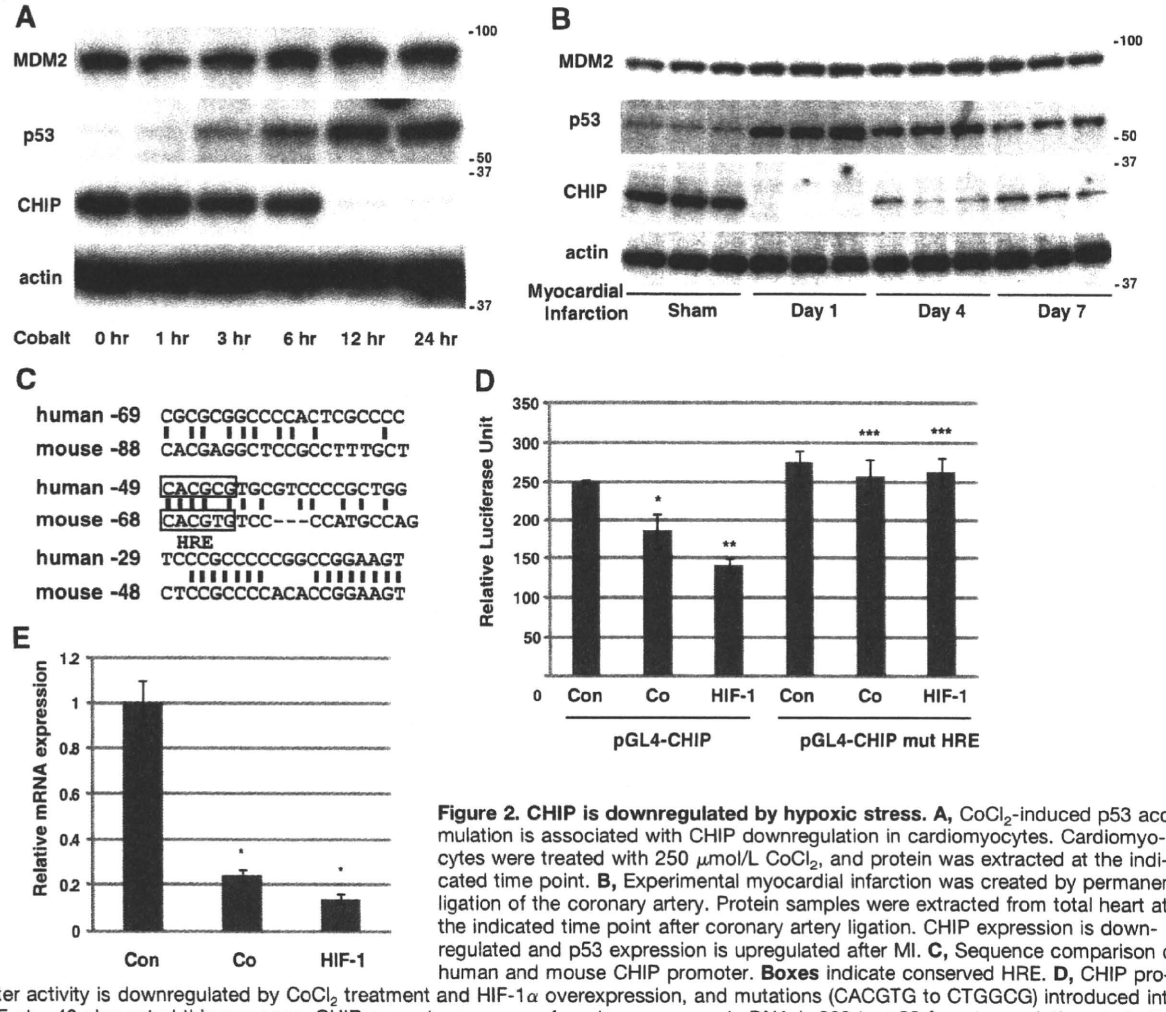

Figure 2. CHIP is downregulated by hypoxic stress. A, $CoCl_2$-induced p53 accumulation is associated with CHIP downregulation in cardiomyocytes. Cardiomyocytes were treated with 250 μmol/L $CoCl_2$, and protein was extracted at the indicated time point. **B,** Experimental myocardial infarction was created by permanent ligation of the coronary artery. Protein samples were extracted from total heart at the indicated time point after coronary artery ligation. CHIP expression is downregulated and p53 expression is upregulated after MI. **C,** Sequence comparison of human and mouse CHIP promoter. **Boxes** indicate conserved HRE. **D,** CHIP promoter activity is downregulated by $CoCl_2$ treatment and HIF-1α overexpression, and mutations (CACGTG to CTGGCG) introduced into HRE at −49 abrogated this response. CHIP promoter sequence from human genomic DNA (−329 to +39 from transcription start site) was cloned upstream of luciferase gene. Mutation was introduced using a kit from Stratagene. Luciferase assay was performed 24 hours after $CoCl_2$ treatment or HIF-1α overexpression. *$P<0.05$, **$P<0.01$, ***P=NS vs control; n=5. **E,** Real-time PCR analysis revealed mRNA level of CHIP was also downregulated by hypoxic stress (Co) and HIF-1α overexpression. RNA was extracted 24 hours after $CoCl_2$ treatment or HIF-1α overexpression. *$P<0.01$.

lated by HIF-1 at the transcriptional level through HRE. Real-time PCR analysis revealed that exposure of cardiomyocytes to $CoCl_2$ (24 hours) and adenoviral overexpression of constitutively active HIF-1α led to marked downregulation of CHIP mRNA levels (Figure 2E), further supporting our data that hypoxic stress downregulates CHIP levels. HIF-1α gene is both required and sufficient for hypoxic stress-induced CHIP downregulation and p53 accumulation because knockdown of HIF-1α attenuated the effects of $CoCl_2$ treatment on expressions of p53 and CHIP (Online Figure III, A), and overexpression of constitutively active HIF-1α suppressed CHIP expression and increased p53 expression in cardiomyocytes (Online Figure III, B). Furthermore, downregulation of CHIP protein levels after MI was attenuated in cardiac-specific inducible HIF-1α conditional knockout mice[16] (Online Figure III, C). Collectively, these findings suggest that CHIP transcription is directly downregulated by hypoxia through HIF-1.

CHIP Protects Cardiomyocytes From Hypoxia-Induced p53-Mediated Apoptosis of Cardiomyocytes

Because hypoxia or p53 overexpression induces apoptotic cell death in cultured cardiomyocytes,[14] we next examined whether hypoxia-induced cardiomyocyte apoptosis is mediated by the HIF-1-CHIP-p53 pathway. $CoCl_2$ treatment (24 hours) induced p53 accumulation and promoted apoptosis of cardiomyocytes as assessed by cleaved poly (ADP-ribose) polymerase (PARP) expression (Figure 3A), Annexin V staining (Figure 3B and 3C), and caspase-3 activity (Figure 3D). $CoCl_2$-induced apoptosis was p53-dependent, because knockdown of p53 in $CoCl_2$-treated cardiomyocytes attenuated hypoxia-induced cell death (Figure 3A through 3D). We next assessed whether overexpression of CHIP could rescue $CoCl_2$-induced apoptosis. Adenovirus-mediated overexpression of CHIP in cardiomyocytes markedly downregulated p53 expression and attenuated apoptosis in $CoCl_2$-treated

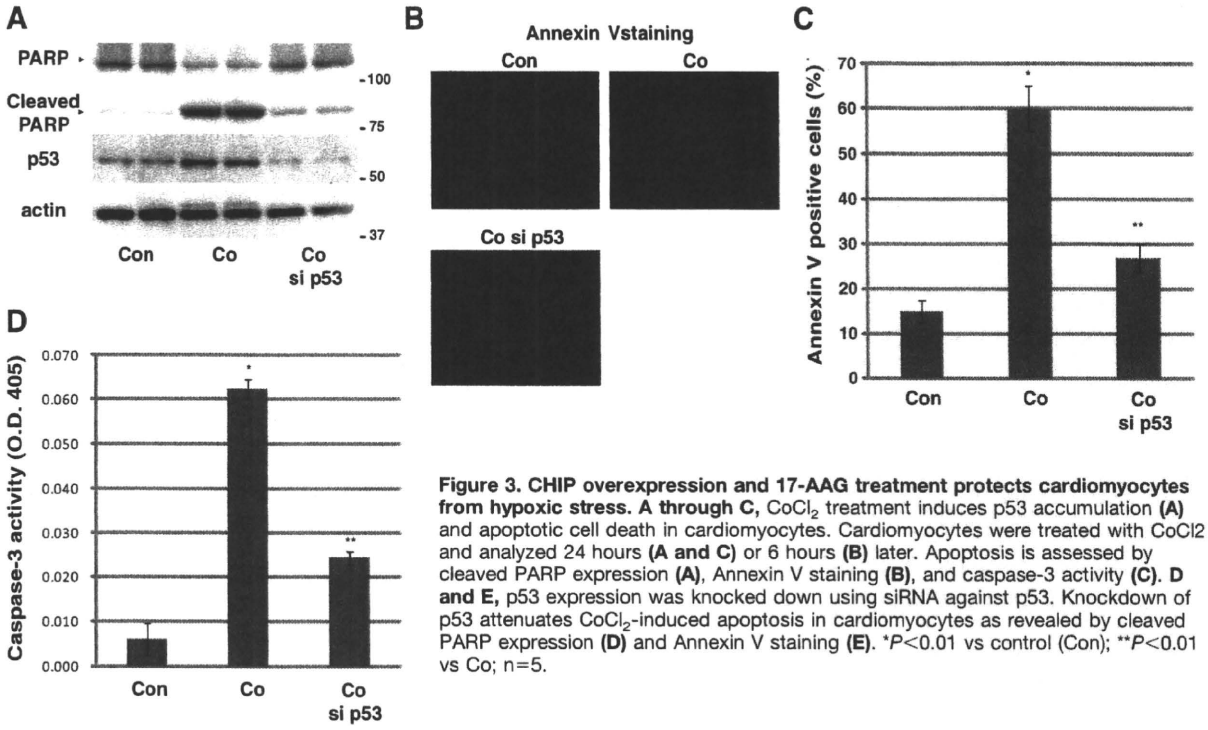

Figure 3. CHIP overexpression and 17-AAG treatment protects cardiomyocytes from hypoxic stress. A through C, $CoCl_2$ treatment induces p53 accumulation **(A)** and apoptotic cell death in cardiomyocytes. Cardiomyocytes were treated with CoCl2 and analyzed 24 hours **(A and C)** or 6 hours **(B)** later. Apoptosis is assessed by cleaved PARP expression **(A)**, Annexin V staining **(B)**, and caspase-3 activity **(C). D and E,** p53 expression was knocked down using siRNA against p53. Knockdown of p53 attenuates $CoCl_2$-induced apoptosis in cardiomyocytes as revealed by cleaved PARP expression **(D)** and Annexin V staining **(E)**. $^*P<0.01$ vs control (Con); $^{**}P<0.01$ vs Co; n=5.

cardiomyocytes (Figure 4A through 4C). These results underscore our hypothesis that downregulation of CHIP is responsible for p53 accumulation after hypoxic stress. Moreover, forced expression of CHIP prevented hypoxia-induced cardiomyocyte apoptosis by inducing degradation of p53, suggesting that CHIP-mediated p53 degradation is a potential therapeutic target.

17-AAG Protects Cardiomyocytes From Hypoxia-Induced Apoptosis

Inhibitors for heat shock protein (Hsp)90 have been shown to promote proteasomal degradation of CHIP client proteins and to be effective for the diseases caused by the accumulation of CHIP substrates.[31,32] We therefore examined whether an Hsp90 inhibitor 17-allylamino-17-demethoxy geldanamycin (17-AAG) induces degradation of p53 protein and protects cardiomyocytes from hypoxic stress. In cardiomyocytes treated with $CoCl_2$, 17-AAG downregulated p53 expression (Figure 4D). 17-AAG treatment also suppressed hypoxia-induced cardiomyocyte apoptosis in a CHIP-dependent manner, because CHIP knockdown attenuated the protective effects of 17-AAG (Figure 4E through 4G). These results suggest that 17-AAG protects cardiomyocytes from hypoxic stress by promoting CHIP-mediated p53 degradation.

Interestingly, protein level of CHIP was increased by 17-AAG treatment (Figure 4E). As mRNA level of CHIP was not changed by 17-AAG treatment (Online Figure IV, A), we speculated that protein stability was affected by 17-AAG treatment. When protein translation was inhibited by cycloheximide, 17-AAG treatment dramatically extended the protein half-life of CHIP (Online Figure IV, B and C). 17-AAG also upregulated the protein stability of other proteins, Hsp70 and HSF-1 (Online Figure IV, B and C). Because 17-AAG exerted some antiapoptotic effects even in the cells of negligible CHIP protein level (Figure 4E and 4F), upregulation of these cardioprotective proteins[33,34] might mediate part of the effects of 17-AAG. It remains to be determined how 17-AAG prolongs protein half-life of certain kinds of proteins.

CHIP and 17-AAG Prevent Apoptosis and Ventricular Remodeling After Myocardial Infarction

We next examined whether promotion of CHIP-mediated p53 degradation could attenuate ischemic cardiac injury also in vivo. For this purpose, transgenic mice which overexpress CHIP specifically in the heart (CHIP-Tg) (Figure 5A) were subjected to permanent coronary artery ligation. In CHIP-Tg mice, elevation of p53 protein levels (Figure 5B) and apoptotic cardiomyocyte death in the border zone of the infarct area (Figure 5B and 5C) were attenuated compared to wild-type littermates at 24 hours after the MI operation. Apoptotic death of the cardiomyocytes in the remote zone of the infarct was not changed between littermates (data not shown). We next examined whether this decrease in apoptotic cell death leads to attenuation of cardiac ventricular remodeling. At day 14, CHIP-Tg mice exhibited smaller heart weight/body weight (HW/BW) ratio, better contractility and less ventricular remodeling (Figure 5D and 5E) compared to wild-type littermates. These results provides an evidence for our hypothesis that CHIP downregulation is responsible for p53 accumulation after myocardial infarction, and suggests that CHIP overexpression is protective for the heart by preventing p53 accumulation and cardiomyocyte apoptosis after myocardial infarction.